SAPIENZA
UNIVERSITÀ DI ROMA

2-hydroxyisobutyric acid (2-HIBA) modulates ageing and fat deposition in *C. elegans* animal model

Facoltà di Scienze Matematiche Fisiche e Naturali
Dipartimento di Biologia e Biotecnologie Charles Darwin
PhD Course in Cell and Developmental Biology XXXV Cycle

Adele Preziosi
Matricola 1328351

Supervisor
Prof. Daniela Uccelletti

A.A. 2021-2022

Index

English summary

2-hydroxyisobutyric acid (2-HIBA) is a metabolite found in human urine. Recent studies have shown that 2-HIBA levels increased in patients with obesity and hepatic steatosis, suggesting that it could potentially be involved in clinical conditions. 2-HIBA is associated with reduced bacterial diversity and the higher levels of *F. prausnitzii* in obese gut microbiota. We investigated how treatment with 2-HIBA affected the physiology of the model organism *Caenorhabditis elegans*, in both standard and High-Glucose Diet (HGD) growth conditions, by targeted transcriptomics, metabolomic analyses, Coherent Anti-Stokes Raman Scattering (CARS) and two-photon fluorescence microscopy.

2-HIBA in both conditions resulted particularly effective to extend the lifespan, delay ageing processes and stimulate the oxidative stress resistance in wild type nematodes through the activation of insulin/IGF-1 signalling (IIS), and p38 MAPK pathways. Lifespan extension was mediated by the activation of SKN-1 transcription factor and moreover by the peptide transporter PEP-2. 2-HIBA pro-longevity effect on *C. elegans* appeared to be correlated to an increase in tryptophan levels as a consequence of a reduced expression of 2,3-dioxygenase (TDO) in treated animals. On the other hand, 2-HIBA influenced lipid metabolism in independent manner: in worms grown without Glucose (No-GD) , 2-HIBA induced an increase in lipid droplets which instead decreased in HGD conditions, suggesting the activation of different pathways. Therefore, this study represents a first step in understanding the impact of 2-HIBA on *C. elegans* animal model.

Italian summary

L'acido 2-idrossiisobutirrico (2-HIBA) è un metabolita trovato nell'urina umana. Recenti studi hanno dimostrato che i livelli di 2-HIBA sono maggiori nei pazienti con obesità e steatosi epatica, suggerendo che potrebbe essere potenzialmente coinvolto in condizioni cliniche. 2-HIBA è associato a una ridotta diversità batterica e alla presenza aumentata di *F. prausnitzii* nel microbiota intestinale obeso. L'obiettivo di questo lavoro è stato quello di studiare come il trattamento con 2-HIBA potesse influenzare la fisiologia dell'organismo modello *Caenorhabditis elegans*, sia in condizioni di crescita standard che ad alto contenuto di glucosio (HGD), mediante analisi trascrittomiche e metabolomiche mirate, Coherent Anti-Stokes Raman Scattering (CARS) e attraverso studi di microscopia a fluorescenza.

2-HIBA in entrambe le condizioni è risultato particolarmente efficace nel prolungare la durata della vita, ritardare i processi di invecchiamento e stimolare la resistenza allo stress ossidativo nei nematodi di tipo *wild type* attraverso l'attivazione dei *pathways* insulina/IGF-1 (IIS) e p38 MAPK. L'estensione della durata della vita è in particolar modo indotta dall'attivazione del fattore trascrizionale SKN-1 e dal trasportatore peptidico PEP-2. L'effetto di pro-longevità del 2-HIBA su *C. elegans,* potrebbe essere inoltre correlato all'aumento dei livelli di triptofano come conseguenza di una ridotta espressione di 2,3-diossigenasi (TDO) negli animali trattati. D'altra parte, 2-HIBA ha influenzato il metabolismo lipidico in modo indipendente; nei vermi cresciuti senza glucosio (No-GD) 2-HIBA ha indotto un aumento delle goccioline lipidiche che invece sono diminuite in condizioni di HGD suggerendo l'attivazione di diverse vie. Questo studio, dunque, rappresenta un primo passo per la comprensione dell'impatto di 2-HIBA nell'organismo modello *C. elegans.*

Synopsis

The effects of complex factors resulting from the interactions between genetics and environment are known to be involved in the aetiology of several multifactorial diseases like diabetes, cardiovascular diseases, cancer, etc. The metabolome of an organism consists of a huge variety of exogenous and endogenous low molecular-weight molecules deriving from a large network of metabolic reactions. Multiple studies indicated that pathological conditions have a relationship with dysregulated metabolic pathways and an aberrant gut microbiota. Obesity is a significant risk factor for some of the major diseases of the last decades, that arises when the energy supply, mainly in form of triglycerides, exceeds its consumption. An important diagnostic role in the development of this metabolic disorder is played by intestinal microbiome which differs in the composition between healthy and obese individuals, mainly in terms of *Firmicutes*/*Bacteroidetes* ratio, which is higher in obese subjects. Metabolic profiling of human urine showed reproducible patterns of metabolite excretion associated with adiposity. In particular, 2-Hydroxyisobutyric acid (2-HIBA), a mammalian urinary metabolite, has been detected at high levels in the urine of obese people and is associated with reduced bacterial diversity and the higher presence of *F. prausnitzii* in obese gut microbiota. It is hypothesized that a dysregulation in glucose and lipid metabolism is to be linked to a higher content of urinary 2-HIBA. However, the molecular relationship between 2-HIBA levels and biological processes are still not known.

The high homology between the genes of *Caenorhabditis elegans* and those implicated in human diseases makes the nematode an important model for the study of human pathologies. *C. elegans* resulted to be a powerful model for studying the molecular mechanisms of signal transduction pathways, such as the oxidative stress and Insulin-insulin like growth factor (IIS) pathway. Moreover, worms can be used to study fat accumulation, through staining of lipid droplets, localized in gut granules and hypodermal cells.

In this project, *C. elegans* was used to understand the molecular and cellular mechanisms underlying the 2-HIBA treatment through genetic, lipidomic and metabolomic approaches in both standard and High-Glucose Diet (HGD) growth conditions.

To better clarify the molecular mechanisms involved in 2-HIBA mediated cell responses, the viability rate was examined in wild-type nematodes grown in standard conditions and supplemented with different concentrations of 2-HIBA. The most pronounced prolongevity effect was observed in worms treated with 10 mM 2-HIBA along with a significant reduction in progeny production, suggesting that worms spent more energy to live longer than to produce progeny. Analysis of the two aging biomarkers *pumping rate* and *lipofuscin accumulation* showed that nematodes supplemented with 10 mM 2-HIBA displayed an increased number of pharynx contractions with respect to the untreated nematodes, both during the stage of young adults and in old ones, and a reduction of lipofuscin accumulation at 11 days of adulthood. These results indicated that 10 mM 2-HIBA treatment had an impact in delaying ageing processes in *C. elegans*. During ageing, oxidative stress increases in *C. elegans*, thus, the transgenic *sod-3*::GFP and *gst-4*::GFP strains were analysed to assess the localization of the two detoxifying enzymes, the superoxide dismutase 3 and glutathione

S-transferase 4, respectively. In this case, treatment with 2-HIBA induced a slight reduction of SOD-3 and GST-4 expression and a reduction in ROS production. It has been reported that pro-longevity and oxidative stress responses in *C. elegans* are induced via the activation of different pathways, such as DAF-2/DAF-16 (IIS) or p38 MAPK cascades. In order to understand possible mechanisms of action mediated by 2-HIBA, a real time qPCR analysis was carried out. Transcripts analysed include those encoding for the insulin-like growth factor 1 (IGF-1) receptor DAF-2, the forkhead box transcription factors class O (FoxO) homolog DAF-16 and the mitogen-activated protein kinase kinase (MAPKK) SEK-1. In worms treated with 10 mM 2-HIBA, we observed an increased transcription of *sek-1* gene and a reduction of genes involved in insulin/IGF-1 signaling (IIS) pathway (*daf-2* and *daf-16*) with respect to the untreated worms. In agreement, 10 mM 2-HIBA supplementation of transgenic *daf-16*::GFP animals showed a reduced nuclear accumulation of the protein. The p38 MAPK pathway is involved in lifespan extension, innate immunity and oxidative stress responses culminating with the nuclear translocation of the transcriptional factor SKN-1, an orthologue of the mammalian Nrf2. Treatment of the animals carrying the GFP fused to the transcriptional factor induced a higher translocation of SKN-1 in nuclei, as compared to the untreated nematodes, while *skn-1* mutants didn't show any extension of the lifespan when supplemented with 2-HIBA. Therefore, these results indicated that pro-longevity effects mediated by 2-HIBA are SKN-1 dependent.

Since ageing is related also to lipid metabolism, the effect of 2-HIBA was evaluated on the accumulation of *C. elegans* lipid reserves. Fluorescence microscopy images of lipid droplets showed that animals supplemented with 10 mM 2-HIBA presented an increase in the accumulation of vesicles in terms of size and number as compared to the control population. This increase in 2-HIBA treated animals correlated with the activation of IIS pathway and the decrease in the expression of *acs-2* gene, coding for a crucial enzyme involved in the fatty acid β-oxidation pathway. These data, along with the enhanced expression of *sams-1*, *sbp-1* and *fat-7* genes involved in lipid biosynthesis, strengthen the evidence that the accumulation of fat storage in treated nematodes was probably due to an imbalance between synthesis and degradation of lipids. It was also evaluated the role of 2-HIBA in obese worms by genetic approaches: specifically, *pep-2* mutants were exploited, since they lack the intestinal di- and tri-peptide transporter involved in worm development and growth, resulting in an obese phenotype. The animals showed an increase of body fat, resistance to oxidative stress, and a reduction in body size and progeny compared to N2 wild-type worms. Unlike N2 strain, 10 mM 2-HIBA administration was not able to prolong life and to increase *sams-1* transcripts in *pep-2* worms. Moreover, regarding lipid metabolism, the slight increase of *acs-2* transcript levels, although significant, did not reach the high values observed for *fat-7* and *sbp-1* synthesis genes, resulting in increased lipid droplets. Overall, these data suggest the requirement of *pep-2* for the 2-HIBA-dependent extension of lifespan.

Glucose is an essential energy source for many cellular processes. The high-glucose diet (HGD) is related to obesity and pathological conditions and it is known to be linked to a higher production of ROS. Indeed, an altered glucose homeostasis negatively influenced the development, fertility and lifespan of organisms such

as yeasts, worms, and mammals. Our results showed that reduced viability in HGD N2 worms was partially restored by 2-HIBA treatment, even if the median lifespan values did not reach the ones observed for worms grown in standard condition (No-GD). The treatment with 2-HIBA also in this case was able to delay aging processes.

Pro-longevity effects and the delay in aging in worms also depend on SKN-1 signalling and on the transcription factor DAF-16, which acts in the IIS pathway. Worms treated with 2-HIBA in HGD condition showed a reduction in transcript levels of *daf-2*, *daf-16* and an increase of *sek-1* transcript levels, as compared to control population. Unlike the No-GD conditions, microscopy analyses on HGD nematodes treated with different concentrations of 2-HIBA revealed a dose-dependent decrease of intestinal and hypodermal lipid droplets, in terms of distribution and morphology. Treatment of HGD worms with 10 mM 2-HIBA showed a further increment in the expression of *sams-1* and *fat-7* genes. However, in these nematodes also *acs-2* levels increased, unlike the reduction observed in No-GD treated animals. This could explain an enhancement in the β-oxidation process, compared to the untreated ones, resulting in a reduction of lipid vesicles. Analysing *pep-2* mutant worms in HGD condition, 2-HIBA didn't have a positive effect to extend lifespan, but it was able to reduce lipid droplets through a significant increase of *acs-2* expression, involved in β-oxidation. These results suggest a role for 2-HIBA in the modulation of lipid metabolism depending on the diet, although further studies are needed to understand the pathway involved.

Preliminary results of metabolomic analysis highlighted a significant increase in tryptophan (Trp) levels in worms treated with 2-HIBA (data not shown). The transcriptional analysis of the *tdo-2* gene, coding for an enzyme able to metabolize free Trp in the kynurenine pathway of Trp degradation, showed that *tdo-2* transcript was lower in 2-HIBA treated worms, as compared to untreated population. This suggests a down-regulated activity of degradation of Trp by 2-HIBA treatment. Therefore, the role of TDO might converge on some of these longevity factors such as DAF-16.

In conclusion, 2-HIBA treatment in both conditions extended lifespan and delayed aging in *C. elegans*. 2-HIBA-mediated lifespan extension occurred through the induction of DAF-16 and SKN-1 signalling pathways and was dependent on *pep-2* gene. However, the role of 2-HIBA in modulating lipid metabolism depends on diet, so further studies are needed to understand the pathway involved. Our data suggest the hypothesis that the presence of 2-HIBA in human urines could be linked to counteracting the accumulation of lipids as a response to a diet characterized by a high carbohydrate content.

Introduction

The effects of complex factors resulting from the interactions between genetics and environment are known to be involved in the aetiology of several multifactorial diseases like diabetes, cardiovascular diseases, cancer, etc. (Arneth et al., 2019; Mi et al., 2020; Guerra et al., 2021). The metabolome of an organism consists of a huge variety of exogenous and endogenous low molecular-weight molecules deriving from a large network of metabolic reactions (Wishart, 2019). It is of great interest to explore the role of specific metabolites or metabolic profiles in the diseases' etiopathogenesis in order to gain insights about their development and progression and on the possible interventional practices. Multiple studies indicated that pathological conditions have a relationship with dysregulated metabolic pathways and an altered gut microbiota (Scheithauer et al., 2020; ve). Metabolites can straightforwardly derive from bacterial metabolic activities, mostly connected to the dietary intake, or from modification of host molecules (Vernocchi et al., 2020b). Different metabolites have been reported to have beneficial effects in promoting the health status of an individual, while others were associated with several pathologies, such as obesity (Newgard, 2012; Porez et al., 2012; Shen et al., 2013; Preidis et al., 2014). Obesity is a significant risk factor for some of the major diseases of the last decades, such as type 2 diabetes, hypertension and some forms of cancer (Pi-Sunyer, 2009), and it arises when the energy supply, mainly in form of triglycerides, exceeds its consumption (Flier, 2004). Genetic predisposition is a key factor along with diet, stage of development, physical activity and age (Gasmi et a., 2021). An important diagnostic role in the development of this metabolic disorder is played by intestinal microbiome which differs in the composition between healthy and obese individuals, mainly in terms of *Firmicutes*/*Bacteroidetes* ratio, which is higher in obese subjects (Magne et al., 2020). The gut microbiota releases metabolites which can cross the intestinal barrier, impacting on host physiology in a complex interplay (Nicholson et al., 2012). The involvement of the microbiome in the energy balance has been further demonstrated through faecal microbiota transplantation studies in mice, in which germ free animals colonized with the microbiota from obese mice showed significantly higher levels of body fat than did mice colonized with the microbiota from lean donors (Turnbaugh, 2006). In addition, a decrease in the bacteria producing butyrate (*Roseburia* and *Faecalibacterium prausnitzii*) has been found in the gut microbiota of patients with type 2 diabetes, compared to that of healthy individuals (Karlsson et al., 2013; Qin et al., 2012). Butyrate, a short chain fatty, is an important mediator of human health and disease. It is associated with molecular signalling between gut microbiota and host, providing major fluxes of carbon from the diet to the host (Morrison and Preston 2016) and also it has an important roles in supporting immune tolerance and maintenance of the gut barrier (Parada Venegas et al., 2019). However, the mechanisms underlying the potential beneficial effects of butyrate on metabolism aren't entirely clear.

Metabolic profiling of human urine showed reproducible patterns of metabolite excretion associated with adiposity. In particular, 2-Hydroxyisobutyric acid (2-HIBA) (Fig. 1), a mammalian urinary metabolite,

identified by ^{1}H NMR spectroscopy, has been detected at high levels in the urine of obese people (Calvani et al., 2010) and is associated with reduced bacterial diversity and the higher levels of *F. prausnitzii* in obese gut microbiota (Li et al., 2008), 2-HIBA seems to originate from the microbial degradation of dietary proteins that escape digestion in the upper gastrointestinal tract (Li et al., 2008), however is still not proven and, furthermore, its presence in humans' and rodents' stools samples has not been found (Preidis et al., 2014**;** Marrocco et al., 2022). The urinary excretion of 2-HIBA has been observed increasing not only in obese subjects but also in alcohol consumers and in pregnant women who developed gestational diabetes mellitus probably related to higher BMI values, as well as in women with healthy pregnancies (Calvani et al., 2010; Diaz et al., 2011; Elliott et al., 2015; Gil et al., 2018; Irwin et al., 2018). Notably, urinary levels of 2-HIBA could be modulated by treatment with probiotic mixture in NAFLD children or by bariatric surgery in super obese individuals (Calvani et al., 2010; Friedrich et al., 2012; Miccheli et al., 2015). Moreover, in obese and in type 2 diabetic mice, an increased urinary excretion of 2-HIBA was observed, possibly correlated to the degradation pathway of valine, leucine and isoleucine, which belong to Branched-Chain Amino Acids (BCAAs) (Li et al., 2017).

2-hydroxyisobutyric acid

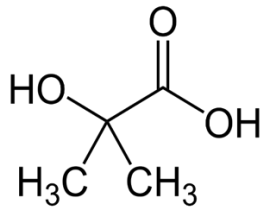

Figure 1. Molecular structure of 2-hydroxyiscobutyruc acid (2-HIBA).

Indeed, among the bioactive molecules involved in nutrition metabolism, BCAAs play mediation roles on protein synthesis, glucose homeostasis, anti-obesity, and nutrient-sensitive signalling pathways (Nie et al., 2018). It has been reported that higher concentrations of circulating BCAAs are associated with an increased risk of type 2 diabetes mellitus (T2DM) and insulin resistance in humans and in some rodent models (Lynch et al., 2014). On these bases, a dysregulation in glucose and lipid metabolism is hypothesized to be linked to a higher content of urinary 2-HIBA and suggests that this metabolite could act as an early biomarker of dysregulated glucose metabolism and an indicator of ketosis. Despite this, the molecular relationship between 2-HIBA levels and biological processes are still not known. However, among the post-translational modifications that regulate transcriptional activity, lysine 2-hydroxyisobutyrylation (K_{hib}) has been identified in bacteria, yeasts, plants and mice (Dai et al., 2014, Huang et al., 2017; Dong et al., 2018; Xue et al., 2020). Consistently, studies in the yeast *Saccharomyces cerevisiae* reported that amount of histone H4K8 2-hydroxyisobutyrylation ($H4K8_{hib}$) were reduced in low-glucose conditions lead to diminished modification

(Huang et al, 2017). The 2-hydroxyisobutyrylome can be considered as a modulator of cell functions through acylation of non-histone proteins regulating some metabolic processes such as tricarboxylic acid cycle, glycolysis and mitochondrial energy metabolism (Huang et al., 2018b, 2018a; Wu et al., 2018; Trefely et al.,2020).

High-glycaemic-index diets in industrialized and emerging countries include a large proportion of processed carbohydrates or sugars, which are readily metabolized to glucose, causing a fast increase in blood glucose level, and altering glucose homeostasis, influencing in a negative way the development, fertility, and lifespan in organisms as diverse as yeasts, worms, and mammals (Alcántar-Fernández et al., 2018). In particular, high-glucose diets (HGD) are known to generate reactive oxygen species (ROS), that include radical and non-radical oxygen species such as hydroxyl radical ($HO^{\cdot}$), superoxide anion ($O_2^{\cdot-}$), and hydrogen peroxide (H_2O_2), which can damage lipids, proteins and nucleic acids and could lead to cell death. For this reason, oxidative stress is considered as a key factor related to the development of several diseases, including obesity and diabetes. High levels of reactive oxygen species (ROS) are intricately linked to obesity and associated pathologies, notably insulin resistance and type 2 diabetes (Murray et al., 2016). The additional energy source in obesity is linked to increased mitochondrial dysfunction and ROS production, which may cause insulin resistance (Houstis et al., 2006).

The high homology between the genes of *Caenorhabditis elegans* (Fig.2) and those implicated in human diseases makes the nematode an important model for the study of human pathologies. *C. elegans* resulted to be a powerful model for studying the molecular mechanisms of signal transduction pathways, such as the oxidative stress and IIS pathways, that influence different human diseases, including diabetes (Moreno-Arriola et al., 2014). The use of this relatively simple organism constitutes an excellent system that can be manipulated through an abundance of powerful cellular, molecular and genetic tools for the discovery of genes involved in various diseases, including obesity (Markaki and Tavernarakis, 2010). Moreover, worms can be used to study fat accumulation, through staining of lipid droplets, localized in gut granules and hypodermal cells (Vrablik et al., 2015).

Figure 2. *Caenorhabditis elegans* animal model (Roselli et al., 2019).

Aim of the study

The multicellular organism *Caenorhabditis elegans* with genome completely sequenced, is an established genetic model organism which possesses homologs for about two-thirds of all human disease genes. The use of *C. elegans* as a model system to recapitulate most human diseases in recent decades is invaluable for experimental research at both the metabolic and genomic levels *in vivo*. Studies using *in vitro* model systems have a limited relevance and *in vivo* studies in vertebrates are time-consuming, cost-intensive, technically challenging, and subject to substantial ethical concerns. Therefore, the use of alternative 3R-compliant *in vivo* test systems such as *Caenorhabditis elegans* is preferable. The 3R principles were designed for animal welfare in science in relation to animal experiments that should be replaced, reduced or refined. Based on its physiological characteristics and superiority, the use of *C. elegans* as a model system for studies on aging, age-related diseases, mechanisms of longevity, and drug screening has been widely acknowledged in recent decades. The use of *C. elegans* in this context will allow to understand the molecular and cellular mechanisms underlying the 2-HIBA treatment through genetics, cellular and molecular biology approaches.

Question to be addressed include how 2-HIBA affects:

- nematode physiology by assessing parameters such as viability, larval development and aging;
- lipid accumulation by observing lipid droplets morphology and associated gene expression;
- oxidative stress, ROS levels and signal transduction pathways;
- metabolites production.

All these targets will be investigated in wild type N2 nematodes and obesity model mutants, treated or not with 2-HIBA in both standard and High-Glucose Diet (HGD) growth conditions. In conclusion, this project represents an opportunity to investigate the role of 2-HIBA in energy metabolism.

Results

2-HIBA delays aging in process in wild-type worms

To better clarify the molecular mechanisms involved in 2-HIBA mediated cell responses, the viability rate was examined on wild-type nematodes, supplemented with increasing concentrations of 2-HIBA, corresponding to 5 mM, 10 mM and 20 mM. The median lifespan of wild type nematodes, fed heat-killed OP50 (OP50 HK) supplemented with 10 mM 2-HIBA from embryo hatching, resulted significantly extended as compared to the untreated controls (Figure 3A). In particular, 50% of worm viability in 10 mM 2-HIBA-supplemented nematodes was recorded at day 22, while in untreated animals it was recorded at day 12. The prolongevity effect was also observed when the supplementation was based on 5 mM or 20 mM 2-HIBA. Indeed, median survival in 5 mM- or 20 mM-supplemented worms was recorded at days 15 and 20, respectively. Therefore, in general the molecule appeared to exert positive effects on *C. elegans* lifespan elongation.

Nematodes' fertility was further analysed evaluating the brood size, expressed as the number of embryos per worm. A significant reduction of progeny production was observed in worms supplemented with all three different concentrations of 2-HIBA, when compared to the control population (Figure 3B). In particular, this reduction was about 40% in animals supplemented with 5 mM 2-HIBA and about 20% in nematodes treated with 10 and 20 Mm 2-HIBA, as compared to worms fed OP50 alone. In order to evaluate possible impact on larval development exerted by the molecule, the larval length was analysed. In this case the treatment with 2-HIBA did not show a particular effect on nematodes' body length, except for a slight reduction in the size of the animals treated with 2-HIBA on the fourth day from hatching (Figure S1). However, this difference seemed to disappear in adulthood, suggesting that the impact of 2-HIBA, observed in *C. elegans* lifespan, did not depend on a delay of larval development.

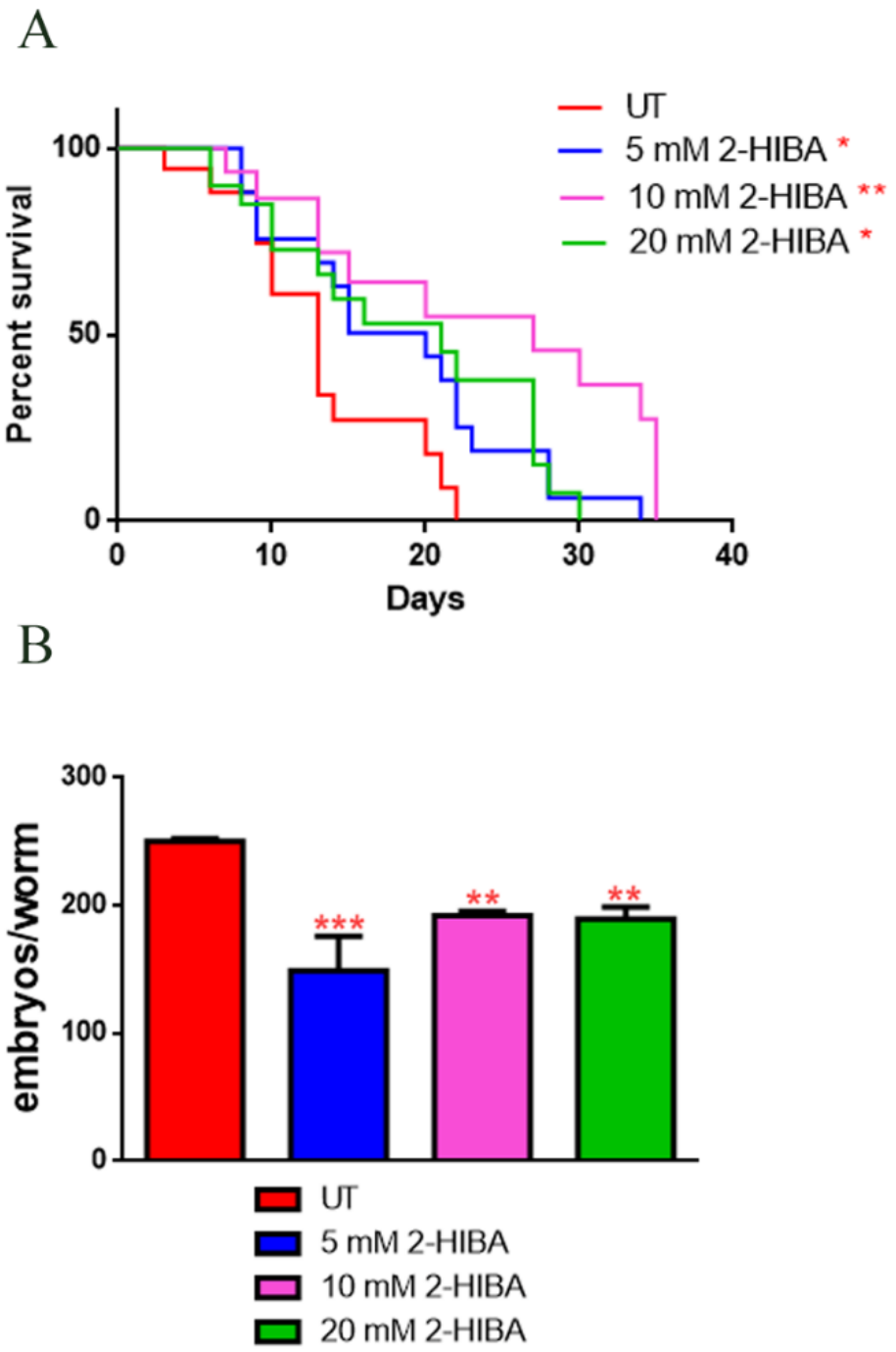

Figure 3. Impact of 2-HIBA on worm viability and fertility. (A) Kaplan–Mèier survival plot of N2 worms fed with heat-killed OP50 and supplemented with 2-HIBA at three different concentrations: 5 mM in blue, 10 mM in pink and 20 mM in green. n = 60 for each data point of single experiments (*p < 0.05, ** p < 0.01). (B) Average embryos production per worm of animals supplemented with different concentrations of 2-HIBA: 5 mM in blue, 10 mM in pink and 20 mM in green. UT: untreated worms. Bars represent the mean of three independent experiments; asterisks indicate the P-values (log-rank test) normalized to the UT (** p < 0.01, *** p < 0.001).

Subsequently, aging biomarkers were analysed in order to evaluate the effects of this molecule on *C. elegans* ageing. To this aim, two ageing markers were considered: pumping rate and lipofuscin accumulation. By measuring contractions of the pharynx, it was observed that nematodes supplemented with 10 mM 2-HIBA displayed an increased number of pharynx contractions with respect to the untreated nematodes, both during the stage of young adults and in old ones (Figure 4A). Moreover, data obtained from the quantification of lipofuscin accumulation showed that at day 11 of adulthood the auto-fluorescent pigment was reduced by about 20% in nematodes supplemented with 10 mM 2-HIBA (Figure 4B and C). These results showed that 10 mM 2-HIBA treatment had an impact in delaying ageing processes in *C. elegans*. Therefore, this concentration was chosen to perform subsequent experiments.

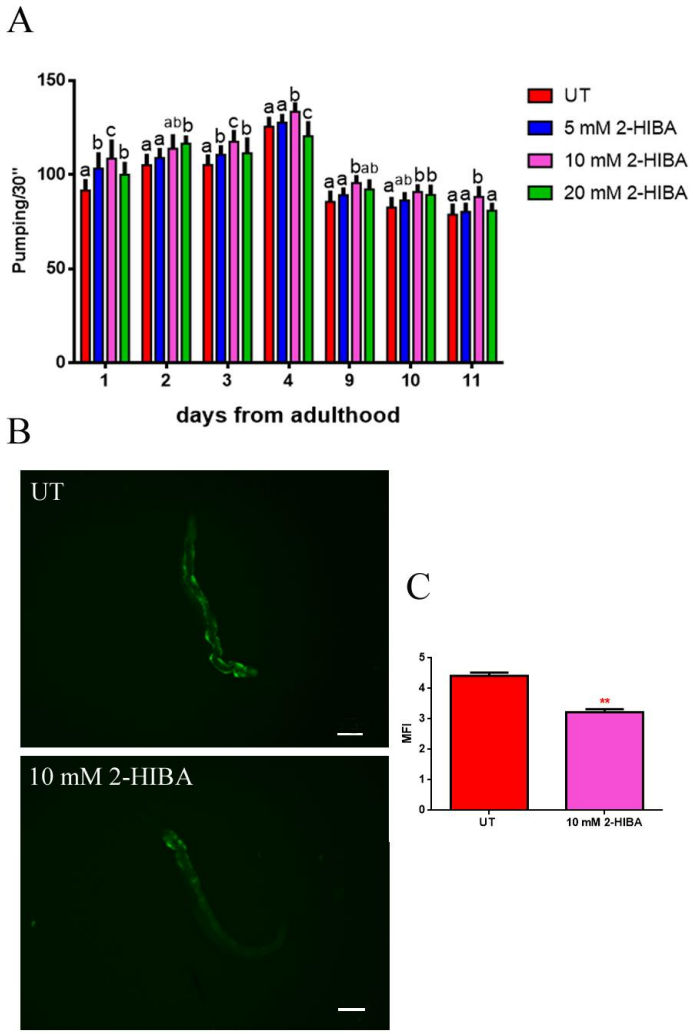

Figure 4. Effect of 2-HIBA on *C. elegans* ageing. (A) Pumping rate of young or old worms measured for 30 s and determined from the mean of 10 worms for each condition. Worms fed heat-killed OP50 without 2-HIBA supplementation were used as controls (UT: untreated). Different letters indicate statistically significant differences ($p < 0.05$). (B) Fluorescence microscopy of auto-fluorescent lipofuscin granules in *C. elegans* supplemented with 10 mM 2-HIBA. (C) Median Fluorescence Intensity related to lipofuscin accumulation. Ten worms were used for each measurement (**$p < 0.01$). Scale bar = 100 μm.

2-HIBA influences oxidative stress response and signal transduction pathways

During ageing, oxidative stress increases in *C. elegans*, thus, the transgenic *sod-3*::GFP and *gst-4*::GFP strains were analysed to assess the expression localizzation of the two detoxifying enzymes, superoxide dismutase (SOD) 3 and glutathione s-transferase (GST) 4. In particular, the *sod*-3 gene codes for a Fe 2+ /Mn 2+ superoxide dismutase present inside the mitochondria and implicated in the defence against oxidative stress through the removal of superoxide radicals (Giglio et al., 1994). The *gst*-4 gene, instead, encodes for a glutathione-S-transferase that requires putative prostaglandins D synthetase and its expression levels increase in response to paraquat (Tawe et al., 1998). In this case, the treatment with 2-HIBA induced a slight reduction of SOD-3 and GST-4 proteins, as confirmed by the quantification of fluorescence by Mean Fluorescence Intensity (MFI) (Figure 5B and D respectively). These results were confirmed analysing *sod-3* and *gst-4* transcripts (Figure 5E).

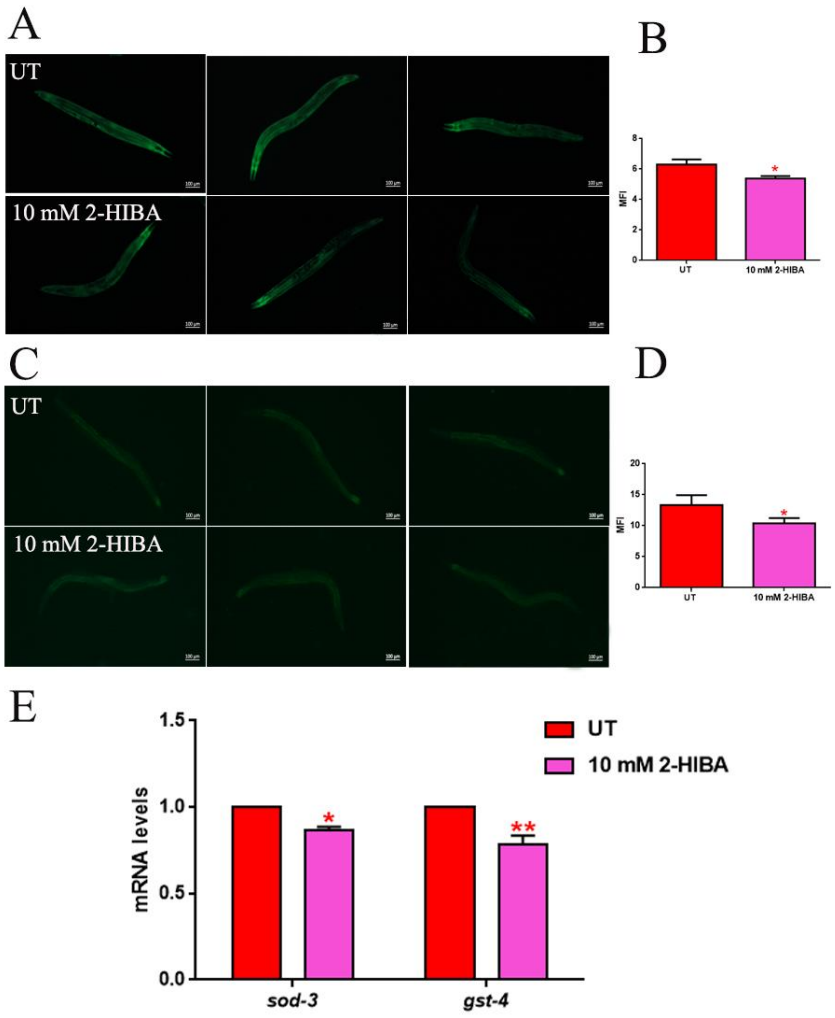

Figure 5. Fluorescence microscopy of *gst-4*::GFP and *sod-3*::GFP transgenic strains. (A) Fluorescence microscopy of *gst-4*::GFP worm strain after supplementation of 10 mM 2-HIBA and (B) related MFI. (C) Fluorescence microscopy of *sod-3*::GFP worm strain after supplementation of 10 mM 2-HIBA and (D) related MFI. Scale bar = 100 μm. (E) Histograms show the expression of *sod-3* and *gst-4* genes detected by real-time PCR. in N2 worms treated with 10 mM 2-HIBA (pink bars) and in untreated nematodes (red bars) at day 1 of adulthood. (*$p < 0.05$, **$p < 0.01$).

Accordingly, in worms supplemented with 10 mM 2-HIBA, ROS levels were 45% lower, as compared to control (Figure 6A-B).

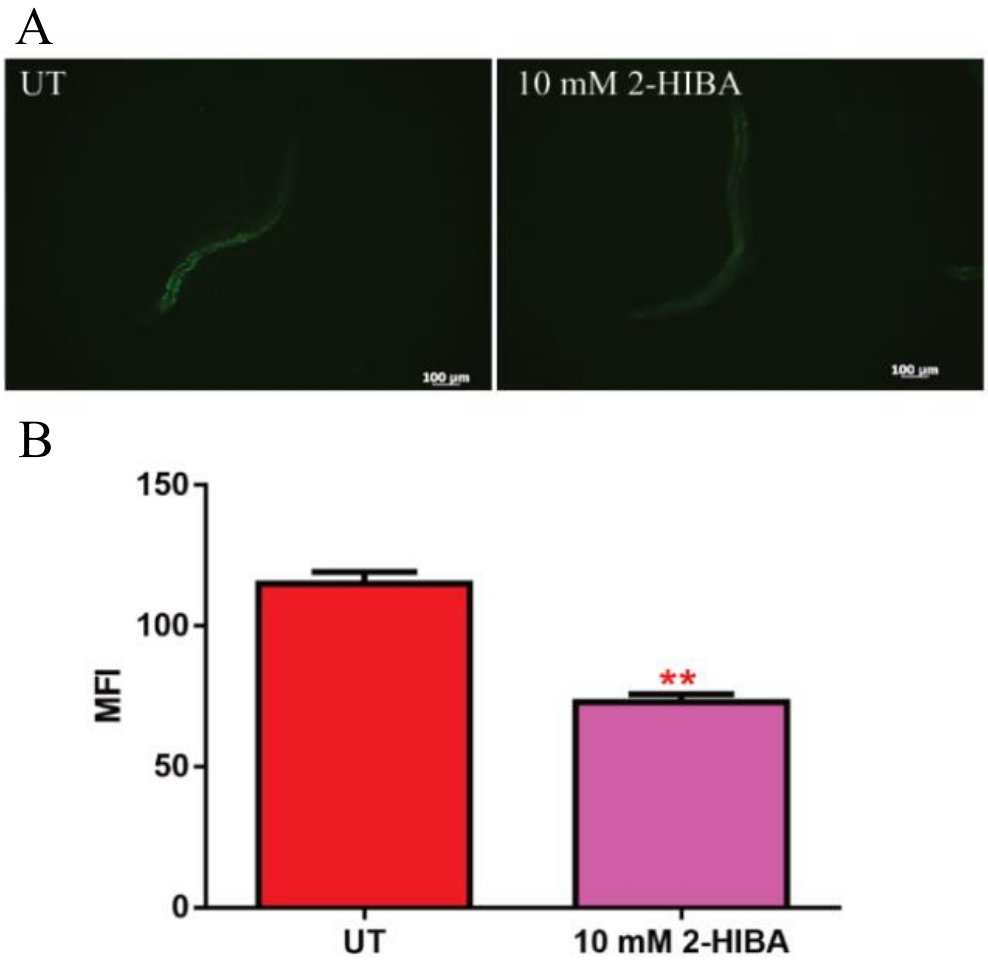

Figure 6. Impact of 10 mM 2-HIBA on oxidative stress response (A) Measurement of ROS levels in supplemented with 10 mM 2-HIBA as compared to untreated control. (B) Relative MFI. Experiments were performed in triplicate. Data are presented as mean ± SD (**$p < 0.01$).

It has been reported that pro-longevity and oxidative stress responses in *C. elegans* are induced via the activation of different pathways, such as DAF-2/DAF-16 (IIS) or p38 MAPK cascades (Roselli et al., 2019). Notably, the IIS pathway starts with the activation of DAF-2 protein, an insulin/insulin-like growth factor-1 receptor orthologue, subsequently beginning a cascade of phosphorylation events that culminate in phosphorylation of DAF-16, a protein belonging to class O of the forkhead transcription factors (FoxO). This modification results in cytoplasmic accumulation of DAF-16 with subsequent inactivation (Sun et al., 2017). Instead, the p38 MAPK pathway is involved in lifespan extension, innate immunity and oxidative stress responses (Kwon et al., 2016; Irazoqui et al., 2010), culminating with the nuclear translocation of the transcriptional factor SKN-1, an orthologue of the mammalian Nrf2 (Nakagawa et al., 2016). In order to understand possible mechanisms of action mediated by 2-HIBA, a real time analysis was carried out.

Transcripts analysed include those encoding for the insulin-like growth factor 1 (IGF-1) receptor DAF-2, DAF-16 and the mitogen-activated protein kinase kinase (MAPKK) SEK-1. Worms treated with 10 mM 2-HIBA showed an increased transcription of *sek-1* gene and a reduced expression of genes involved in insulin/IGF-1 signaling (IIS) pathway (*daf-2* and *daf-16*) with respect to the untreated worms (Figure 7).

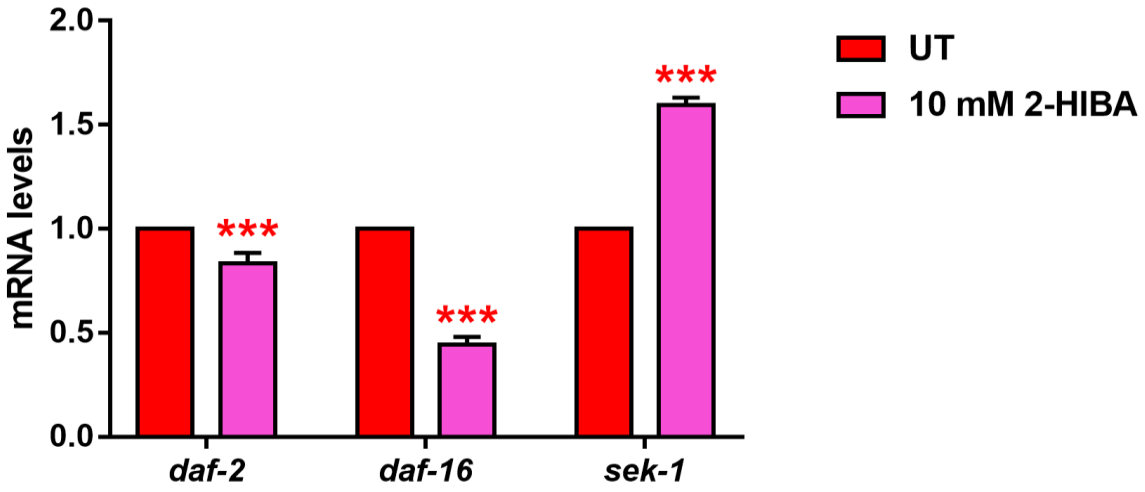

Figure 7. Impact of 10 mM 2-HIBA on signal transduction pathways. Expression of *daf-2*, *daf-16* and *sek-1* genes in N2 worms treated with 10 mM 2-HIBA (pink bars) and in untreated nematodes (red bars) at day 1 of adulthood. Histograms show the expression of genes detected by real-time PCR. Experiments were performed in triplicate. Data are presented as mean ± SD (***$p < 0.001$).

Consistently, 10 mM 2-HIBA supplementation of *daf-16*::GFP and *skn-1*::GFP transgenic animals highlighted the involvement of p38 MAPK cascade and IIS pathway. Indeed, 1 day adult worms fed 2-HIBA 10 mM showed a reduced nuclear accumulation of DAF-16 by 70% as compared to the untreated nematodes (Figure 8A and B), indicating the activation of IIS pathway.

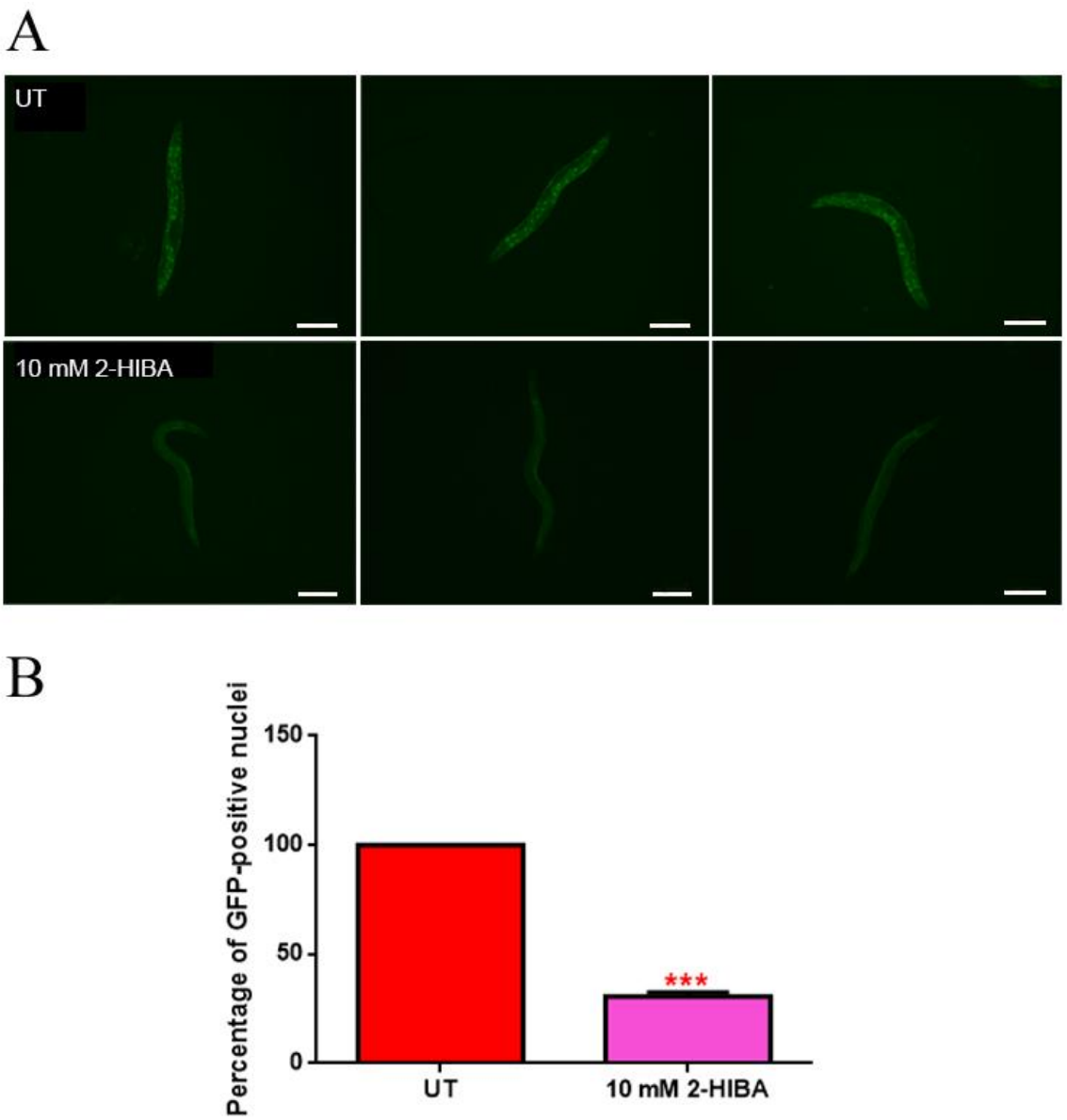

Figure 8. Fluorescence analysis of *daf-16*::GFP transgenic strain. (A) Effect of 10 mM 2-HIBA treatment on localization of DAF-16 protein and (B) respective Median Fluorescence Intensity evaluation. Data were obtained from three independent experiments (60 worms for each condition). Scale bar = 100 μm. UT: untreated nematodes. Statistical analysis was performed by one-way ANOVA with the Bonferroni post-test; asterisks indicate significant differences (***$p < 0.001$). Bars represent the mean of three independent experiments.

On the contrary, after the 2-HIBA administration to *skn-1*::GFP transgenic worms, a higher translocation of the p38 MAPK transcriptional factor SKN-1 was observed in nuclei, as compared to the control population. In particular, in treated nematodes the translocation resulted 2-fold higher than in the untreated ones (Figure 9A and B). Therefore, these results indicated that pro-longevity effects mediated by 2-HIBA could be SKN-1 dependent.

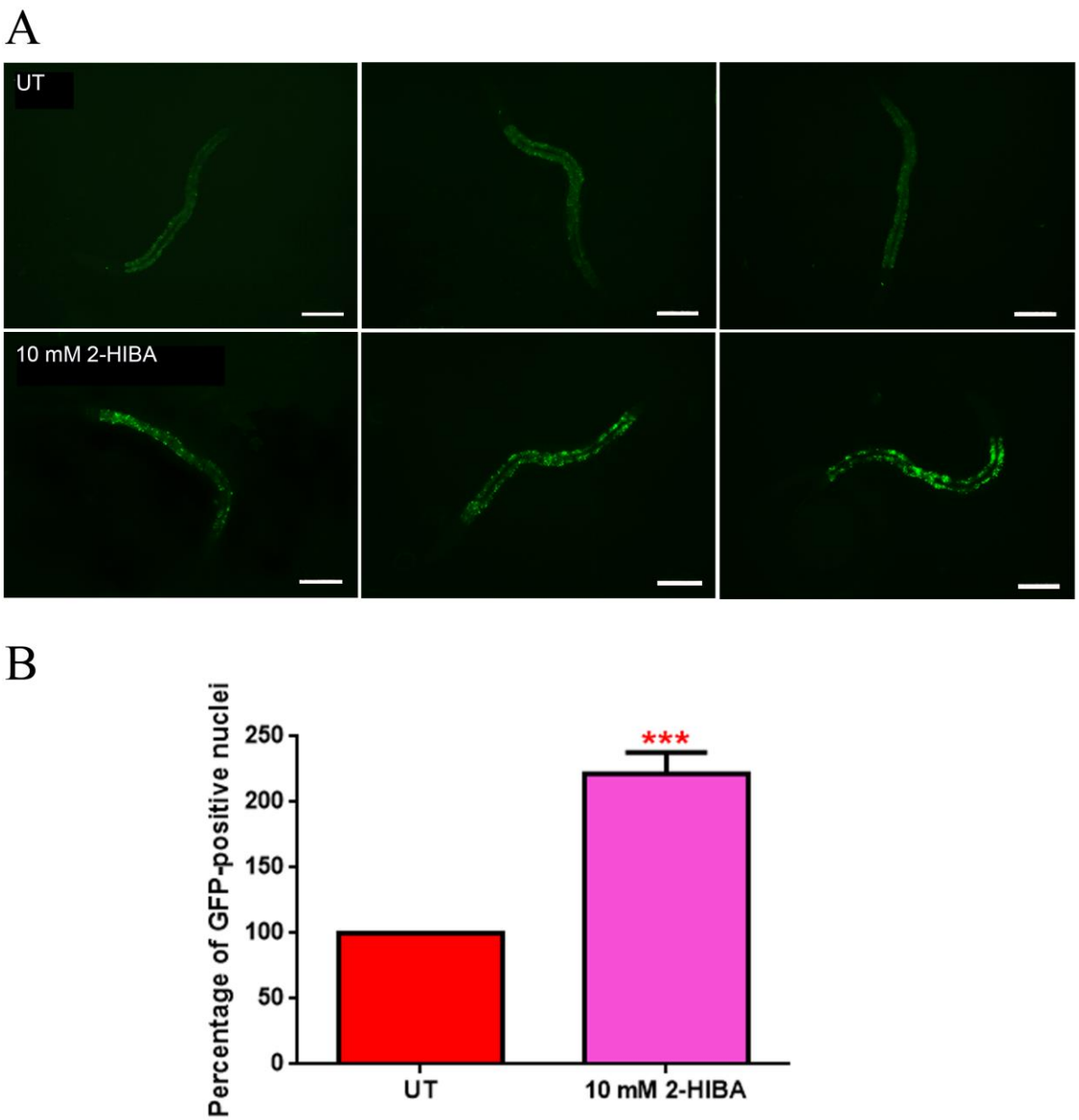

Figure 9. Fluorescence analysis of *skn-1*::GFP transgenic strain. (A) Effect of 10 mM 2-HIBA treatment on localization of SKN-1 transcriptional factor and (B) respective Median Fluorescence Intensity evaluation. Scale bar = 100 μm. Data were obtained from three independent experiments (60 worms for each condition). UT: untreated worms. Statistical analysis was performed by one-way ANOVA with the Bonferroni post-test; asterisks indicate significant differences (***p<0.001). Bars represent the mean of three independent experiments.

To further support these results, the viability rate was further examined by administering 10 mM 2-HIBA to worms with mutations in *pmk-1*, *sek-1* and *skn-1* genes, encoding for proteins involved in p38 MAPK pathway (Nakagawa et al., 2016). The median lifespan of *pmk-1* nematodes, supplemented with 10 mM 2-HIBA from embryo hatching, resulted similar to that of the untreated controls (Figure 10A). In particular, 50% of worm

viability in 10 mM 2-HIBA-supplemented nematodes was recorded at day 12, compared to controls in which, instead, it was recorded at day 13. A similar effect was also observed when the supplementation was added on *sek-1* mutant worms. Indeed, median survival in 10 mM 2-HIBA or untreated *sek-1* worms was recorded at day 12 and day 13, respectively (Figure 10B). In the case of *skn-1* mutants, lifespan reached 50% of viability at day 11 in both conditions (Figure 10C). Therefore, the molecule did not induce a pro-longevity effect in those mutants as observed in wild type animals, demonstrating that the effects mediated by 10 mM 2-HIBA involved the activation of p38 MAPK pathway. These data are in agreement with a previous work showing that *C. elegans* p38 MAPK pathway regulates nuclear localization of the transcription factor SKN-1 in oxidative stress response (Inoue et al., 2005).

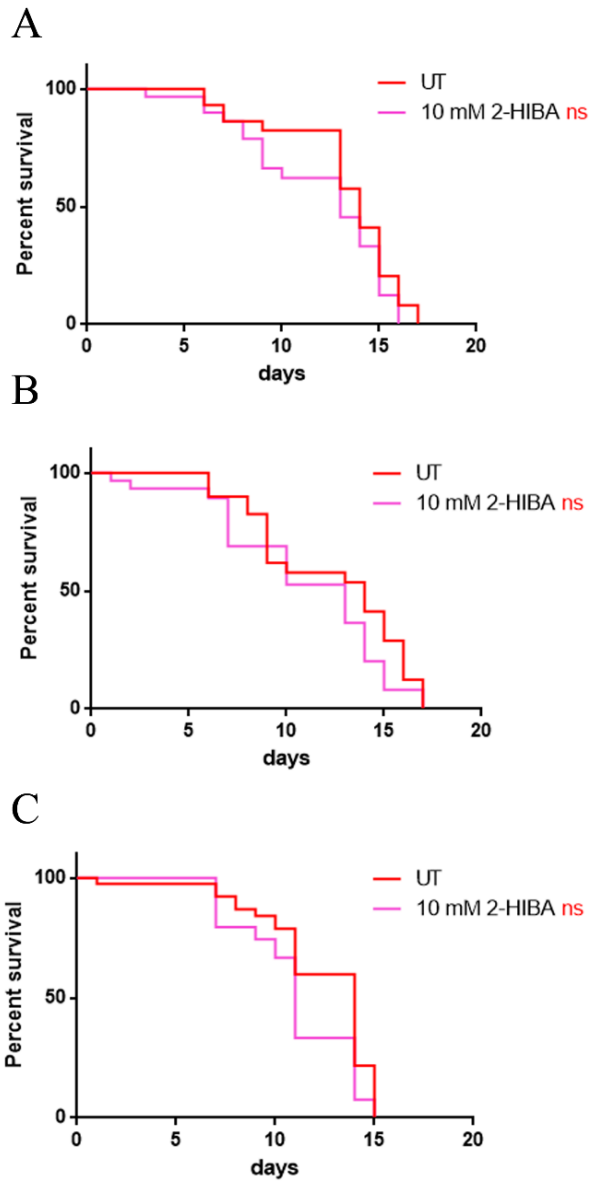

Figure 10. Effect of 10 mM 2-HIBA on *pmk-1*, *sek-1* and *skn-1* mutant animal viability. (A) Kaplan-Meier survival plot of (A) *pmk-1*, (B) *sek-1*, (c) *skn-1* mutant worms supplemented with 10 mM 2-HIBA. Lifespans of untreated worms (UT) were reported as controls; n = 60 for each data point of single experiments (ns: not significant).

2-HIBA induces an increase in lipid accumulation

Since ageing is related also to lipid metabolism, the effect of 2-HIBA was evaluated on the accumulation of *C. elegans* lipid reserves using the BODIPY fluorescent dye. The test was carried out on wild type *C. elegans* treated with 10 mM 2-HIBA and untreated (Figure 11). Images of fluorescence microscopy and lipid droplets quantification showed that animals supplemented with 10 mM 2-HIBA presented an increase in the accumulation of lipid droplets of about 60%, as compared to the control population. In particular, a more pronounced fluorescent signal highlighted an increase in lipid droplets both in size and in number with respect to the control.

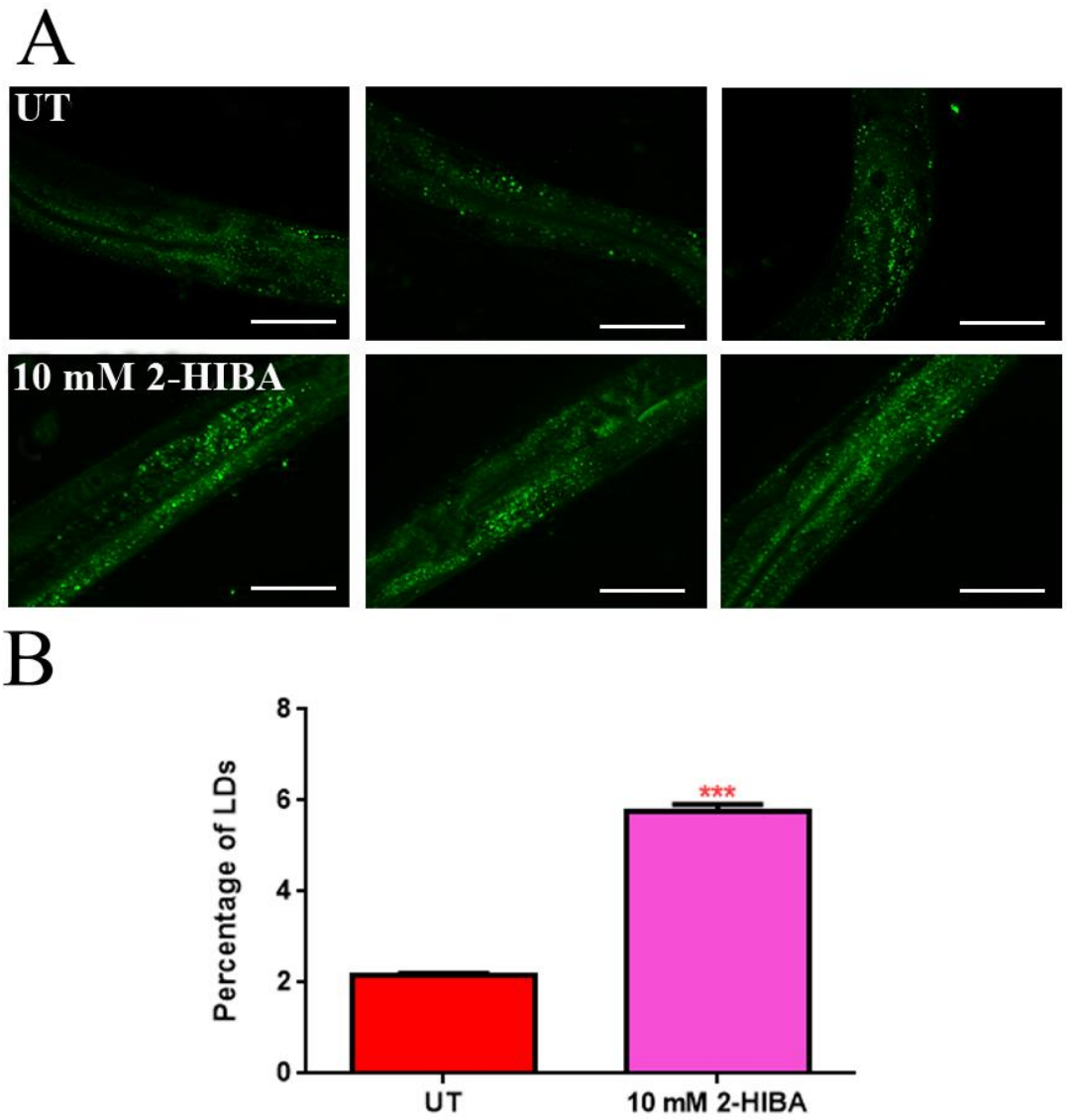

Figure 11. Visualization of lipid droplets. (A) BODIPY staining of 1 day adult worms treated or not with 10 mM 2-HIBA (UT: untreated). Scale bar = 50 μm. (B) Related percentage of lipid droplets. Statistical analysis was evaluated by one-way ANOVA with the Bonferroni post-test; asterisks indicate significant differences (***$p < 0.001$). Bars represent the mean of three independent experiments.

To identify the responsible genes for the differences in fat storage induced by 10 mM 2-HIBA, a real-time qPCR analysis was performed. The genes analysed were S-adenosylmethionine synthetase (*sams-1*), relevant for the synthesis of Phosphatidylcholine (PC); the homolog of the mammalian transcription factor SREBP-1c (*sbp-1*), which facilitates fat storage in mammals (Ehmke et al. 2014); Delta9-fatty acid desaturase (*fat-7*) involved in the biosynthesis process of fatty acids (Watts & Browse, 2000); acyl-CoA synthetase (*acs-2*) that catalyses the conversion of fatty acids into acyl-CoA for the mitochondrial β-oxidation (Van Gilst et al., 2005). The results showed that 2-HIBA induced an increased transcription of *sams-1*, *sbp-1* and *fat-7* genes related to the synthesis of lipids and a reduction of *acs-2*, required for the mitochondrial β-oxidation, as compared to control (Figure 12). In particular, animals supplemented with 10 mM 2-HIBA presented an increased transcription of about 80% for *sbp-1*, 30% for *fat-7* and 50% for *sams-1* and a reduction of 20% for *acs-2*, with respect to control. The results showed an increasing effect of 2-HIBA on synthesis of fatty acids and a decreasing effect on degradation of fatty acids in wild type nematodes.

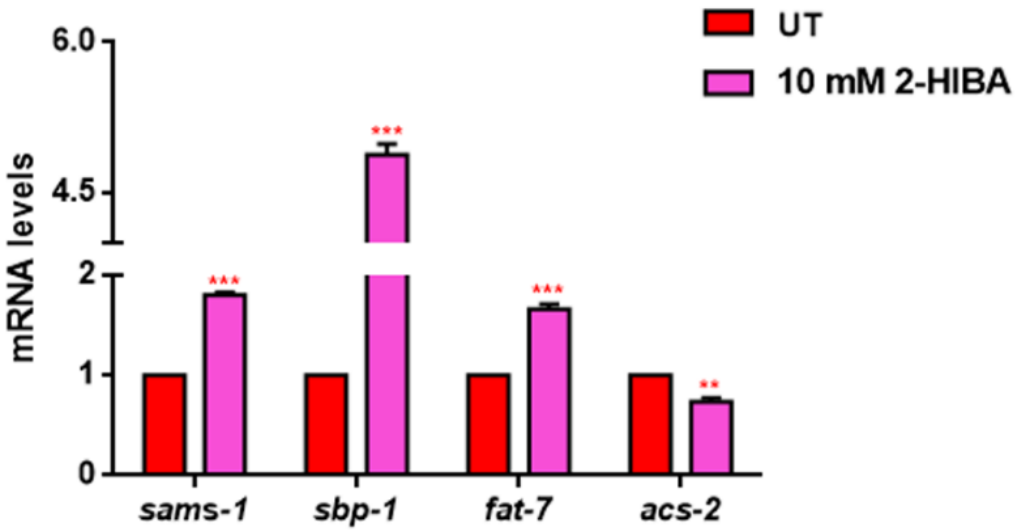

Figure 12. Real time-qPCR analysis of lipid metabolism genes in wild-type worms. Expression of *sams-1*, *sbp-1*, *fat-7*, and *acs-2* genes in 1 day adults treated or not with 10 mM 2-HIBA (UT: untreated). Histograms show the expression of genes involved in lipid metabolism detected by real-time PCR. Experiments were performed in triplicate. Data are presented as mean ± SD (**$p < 0.01$, ***$p < 0.001$).

PEP-2 is involved in 2-HIBA responses

It has been reported that one of the major genes involved in obesity is PEP-2, an intestinal proton-coupled peptide transporter (also known as PEPT-1 in mammals), which mediates amino acid absorption in the form of di- and tripeptides (Meissner et al., 2004). Transporter-deficient animals *(pept-1(lg601))* show impaired growth and metabolic alterations that culminate in a two-fold increase in total body fat content (Zhao et al., 2017). The effects of 10 mM 2-HIBA on obese animals were therefore investigated. As shown in Figure 13A, the treatment of 10 mM 2-HIBA in *pep-2* mutants led to an effect on lifespan similar to that observed on untreated nematodes. Indeed, the median survival of mutant worms was recorded at day 13 for both the conditions. Furthermore, fat accumulation in 10 mM 2-HIBA-fed *pep-2* mutants was about 50% higher than those detected in the untreated population (Figure 13B and C). To analyse fat metabolism gene expression in obesity model, a real time q-PCR was performed on *pep-2* mutants (Figure 13D). Nematodes showed a significant increase of *sbp-1* and *fat-7* mRNA levels when treated with 2-HIBA, while variations in *acs-2* and *sams-1* expression levels were not significant. In particular, *pep-2* mutants supplemented with 10 mM 2-HIBA revealed an increased transcription of about 40% for *sbp-1*, 50% for *fat-7* as compared to untreated worms. Taken together, these results suggested the PEP-2 involvement in responses mediated by 2-HIBA.

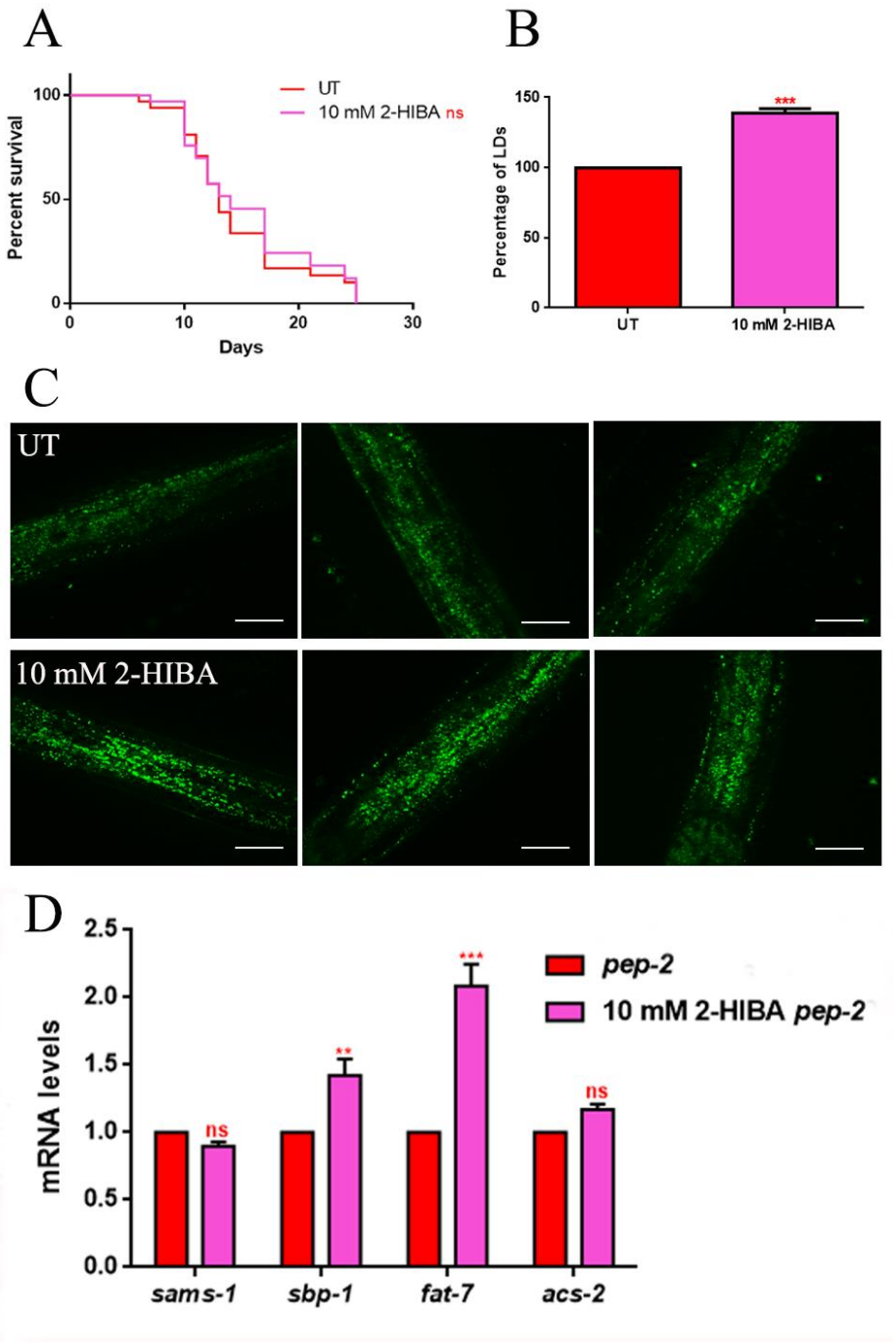

Figure 13. Lifespan analysis and fat accumulation in *pep*-2 mutants. (A) Kaplan-Meier survival plot of *pep-2* mutant worms supplemented with 10 mM 2-HIBA. Lifespans of untreated (UT) worms were reported as controls; n = 60 for each data point of single experiments (ns: not significant). (B) Median Fluorescence Intensity (MFI) of fat accumulation observed by BODIPY staining. Statistical analysis was evaluated by one-way ANOVA with the Bonferroni post-test; asterisks indicate significant differences (***p<0.001). Bars represent the mean of three independent experiments. (C) BODIPY staining of 1-day adult *pep-2* worms treated or not with 10 mM 2-HIBA. Scale bar = 50 µm. (D) Expression of *sams-1*, *sbp-1*, *fat-7*, and *acs-2* genes in 10 mM 2-HIBA-fed 1 day adults. Histograms show the transcript levels of genes involved in lipid metabolism in *pep-2* mutants, supplemented with 10 mM 2-HIBA (purple), as compared to untreated control (red). Experiments were performed in triplicate. Data are presented as mean ± SD (**p < 0.01, ***p < 0.001, ns: not significant).

2-HIBA suppresses negative effects of high-glucose diet

Moreover, it has been reported that high-glucose diet (HGD) affects growth, fertility, ageing and lifespan. Thus, it was investigated whether 2-HIBA was able to counteract glucose toxicity by testing different concentrations of 2-HIBA in wild type animals exposed to 2% glucose. Untreated worms showed a decrease of viability in HGD conditions and median survival at day 5 (Figure 14, UT in red). On the contrary, 2-HIBA supplementation partially restored the worm's lifespan. In particular, in worms treated with 5 mM of 2-HIBA, the 50% of viability was reached at day 10 (Figure 12, 5 mM in blue). In worms treated with 10 mM or 20 mM of 2-HIBA was recorded a median viability at day 7 (Figure 14, 10 mM in purple and 20 mM in green).

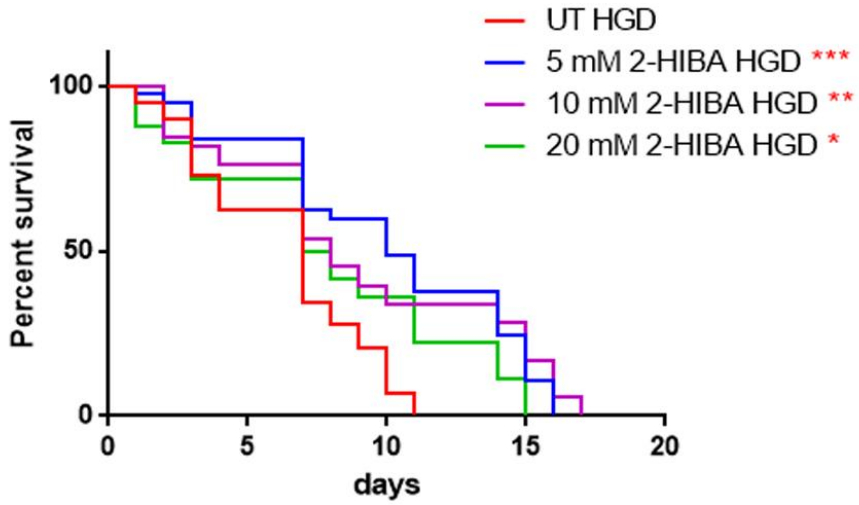

Figure 14. Effect of 2-HIBA on HGD wild-type worm viability. (A) Kaplan–Mèier survival plot of HGD worms treated or not with 2-HIBA at different concentrations (UT: untreated). n = 60 for each data point of single experiments. Bars represent the mean of three independent experiments. Asterisks indicate the P-values (log-rank test) with respect to the untreated control (*$p < 0.05$, **$p < 0.01$, ***$p < 0.001$).

To investigate whether the pro-longevity effects exerted by 2-HIBA positively correlated to a delay in aging also in HGD conditions, pumping and lipofuscin biomarkers were analysed. Figure 15 A showed that 10 mM 2-HIBA supplemented worms share a significantly high pumping rate, at 11 days of adulthood as compared to control. The data obtained from the quantification of lipofuscin accumulation also confirmed this result. In particular, nematodes supplemented with 10 mM 2-HIBA showed, at the stage of 11-days of adulthood, a reduction of about 10% of the autofluorescent pigment, as compared to control population (Figure 15 B and C).

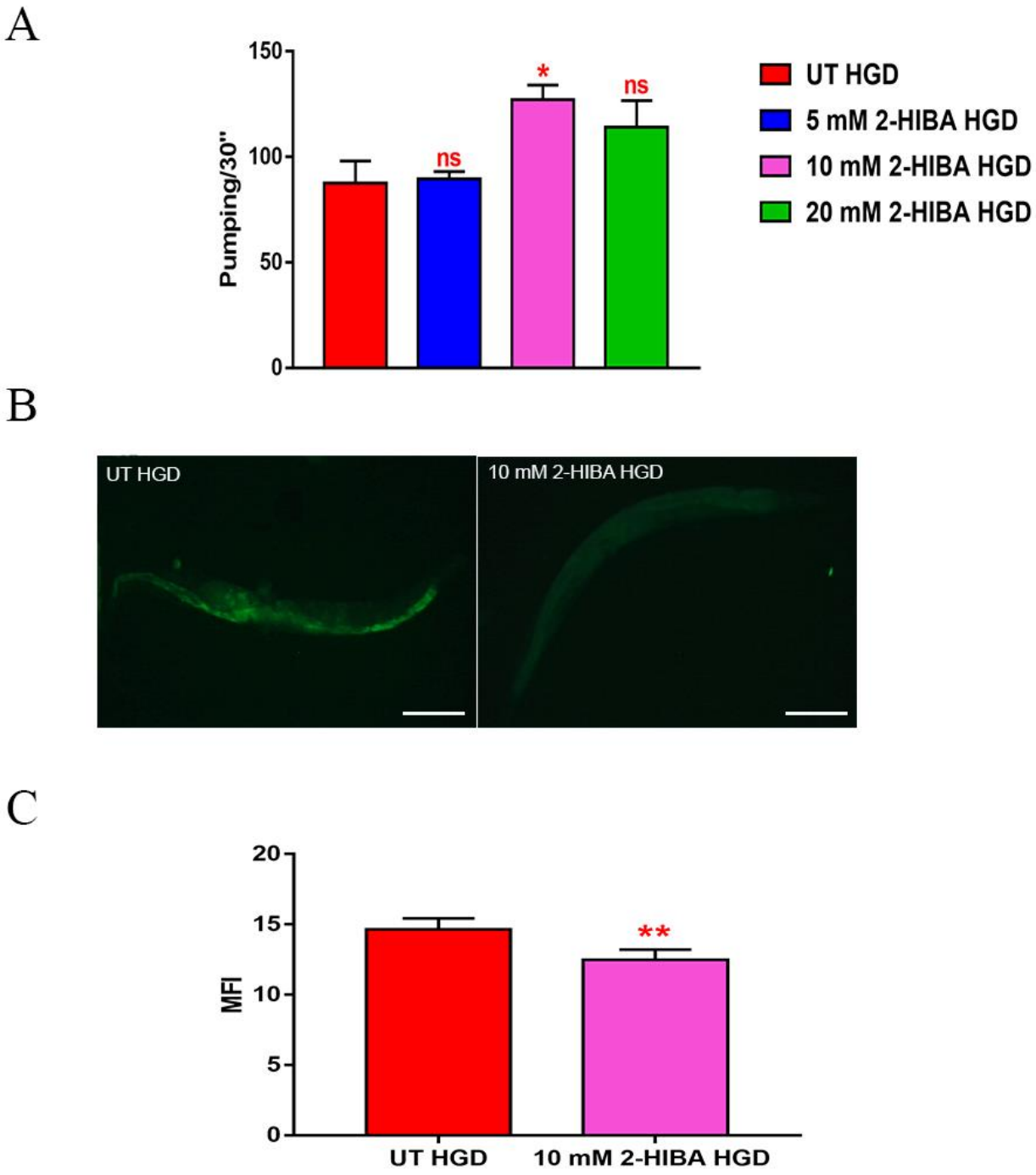

Figure 15. Effect of 2-HIBA on HGD worm ageing. (A) Pumping rate of 11 days-old worms measured for 30 s and determined from the mean of 10 worms for each condition in the presence of glucose. Worms fed heat-killed OP50 without 2-HIBA supplementation were used as controls (UT: untreated). Bars represent the mean of three independent experiments. Statistical analysis was performed by one-way ANOVA with the Bonferroni post-test; asterisks indicate significant differences (*$p<0.05$, ns: not significant). (B) Fluorescence microscopy of auto-fluorescent lipofuscin granules in *C. elegans* supplemented with 10 mM 2-HIBA. Scale bar = 100 μm. (C) Median Fluorescence Intensity (MFI) related to lipofuscin accumulation. Ten worms were used for each measurement (**$p < 0.01$).

To investigate possible 2-HIBA modulation on HGD nematodes on DAF-2/DAF-16 (IIS) and p38 MAPK cascades, transcript levels were analysed for *daf-2*, *daf-16* and *sek-1* genes. The supplementation of the molecule led in worms treated with 10 mM 2-HIBA an increased transcription of *sek-1* gene, a reduction of genes involved in insulin/IGF-1 signalling (IIS) pathway (*daf-2* and *daf-16*) as compared to control population (Fig.16).

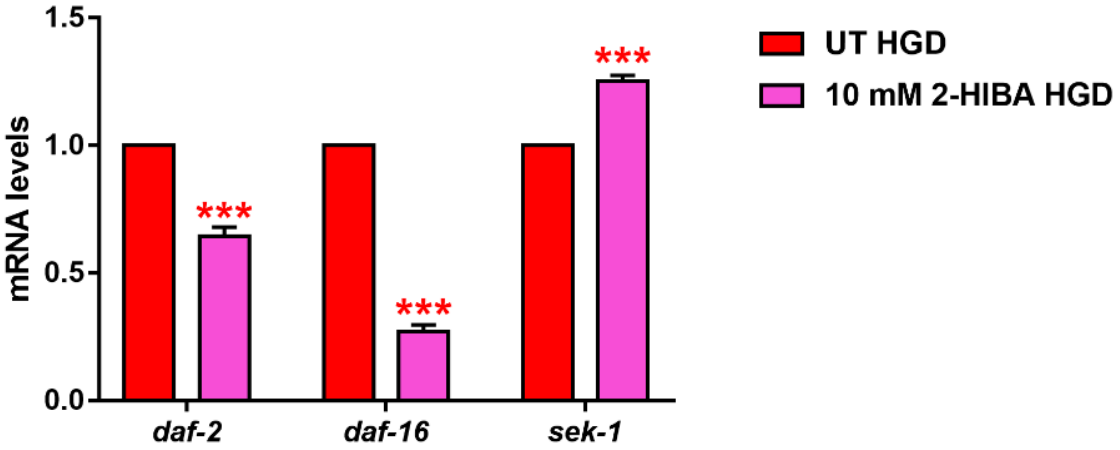

Figure 16. Impact of 10 mM 2-HIBA on signal transduction pathways in HGD worms. Expression of *daf-2*, *daf-16* and *sek-1* genes in N2 worms treated with 10 mM 2-HIBA (pink bars) and in untreated nematodes (red bars) at day 1 of adulthood in the presence of glucose. Histograms show the expression of genes detected by real-time PCR. Experiments were performed in triplicate. Data are presented as mean ± SD (***$p < 0.001$).

Accordingly, 2-HIBA supplementation in *daf-16*::GFP transgenic animals showed that 1-day adult HGD worms fed with 10 mM 2-HIBA had a reduced nuclear accumulation of DAF-16 by 60% (Figure 17A and B) as compared to untreated population. This phenomenon indicated that also for HGD nematodes lifespan extension could be mediated by the activation of IIS cascade.

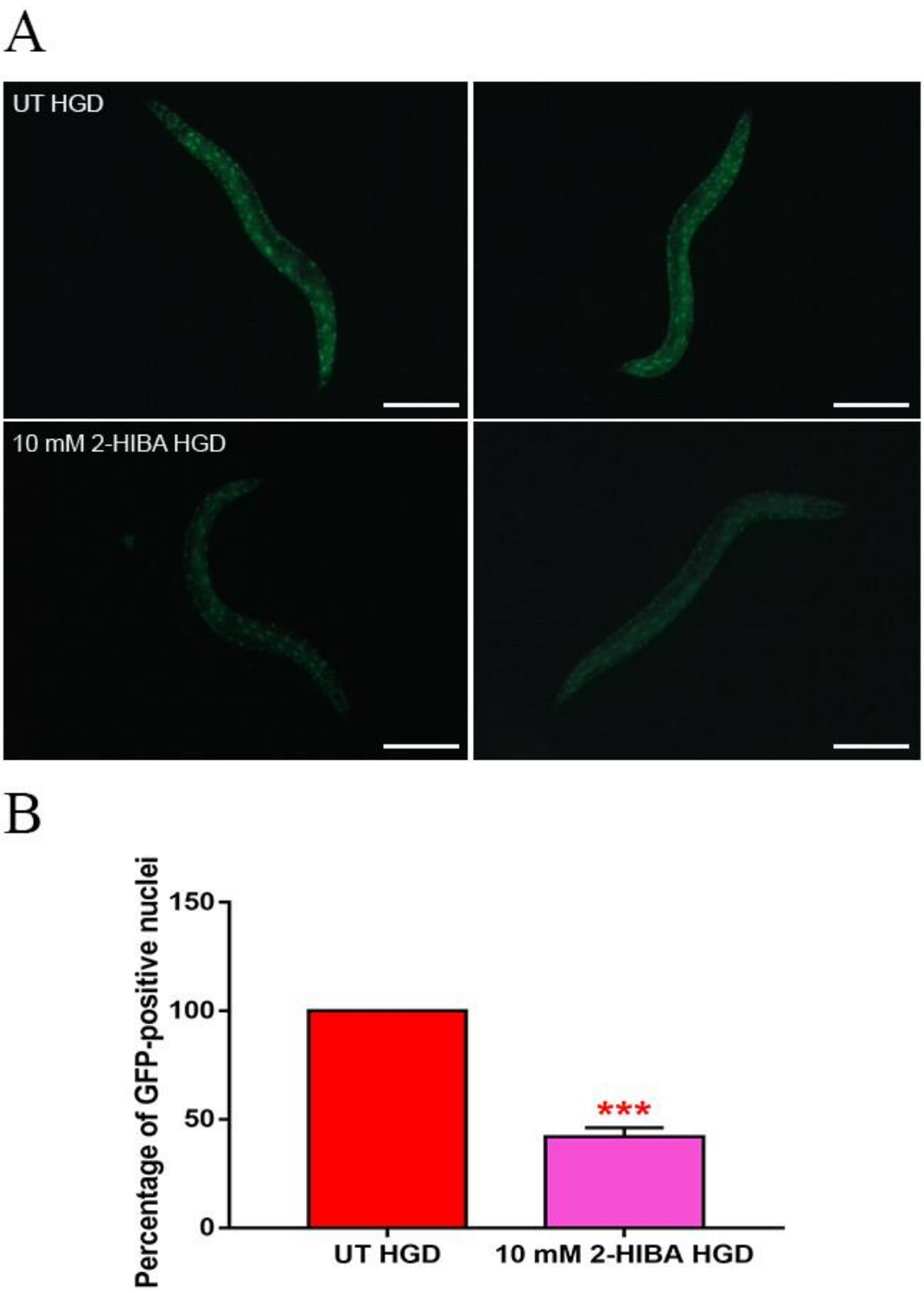

Figure 17. Fluorescence analysis of HGD *daf-16*::GFP transgenic strain. (A) Effect of 10 mM 2-HIBA treatment on localization of DAF-16 protein and (B) respective Median Fluorescence Intensity evaluation. Data were obtained from three independent experiments (60 worms for each condition). Scale bar = 100 μm. UT HGD: untreated nematodes. Statistical analysis was performed by one-way ANOVA with the Bonferroni post-test; asterisks indicate significant differences (***$p < 0.001$). Bars represent the mean of three independent experiments.

On the contrary, after administration of the molecule to *skn-1*::GFP transgenic worms in the presence of glucose, a higher translocation of the transcriptional factor SKN-1 was observed in nuclei, as compared to control. In particular, translocation in 10 mM 2-HIBA HGD nematodes resulted 50% higher than that in control worms (Figure 18A and B) To further support these results, the viability rate was further examined by administering 10 mM 2-HIBA to worms with mutation in *skn-1* gene. The median lifespan of *skn-1* mutant worms, supplemented with 10 mM 2-HIBA from embryo hatching, resulted similar to that of the HGD untreated controls (Figure 18c). These results indicated that prolongevity effects mediated by 2-HIBA could be SKN-1 dependent. Therefore, as in No-GD worms, these results suggested that the metabolite could be involved in the activation of p38 MAPK pathway.

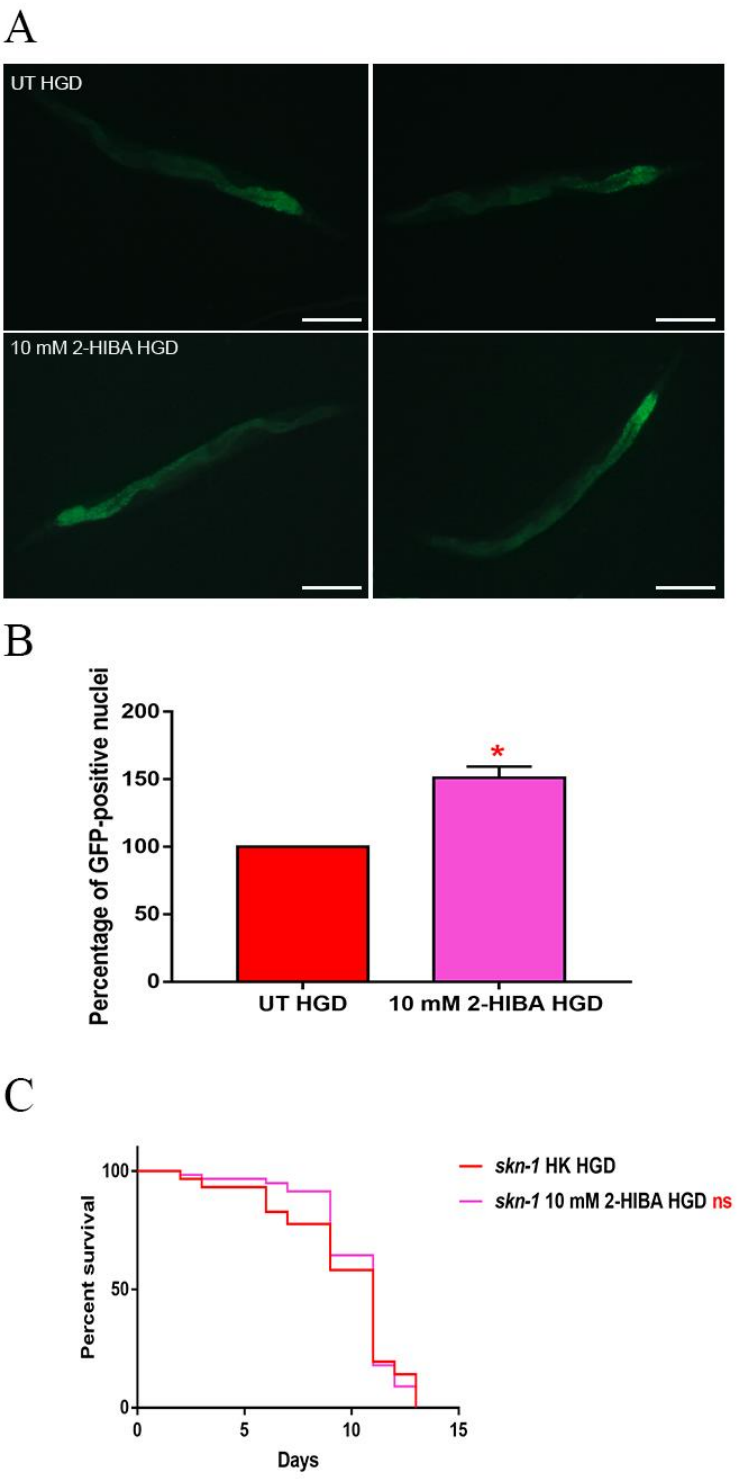

Figure 18. Fluorescence analysis of *skn-1*::GFP transgenic strain and effect of 10 mM 2-HIBA *skn-1* mutant animals in HGD conditions. (A) Effect of 10 mM 2-HIBA treatment on localization of SKN-1 transcriptional factor and (B) respective Median Fluorescence Intensity evaluation. Scale bar = 100 μm. Bars represent the mean of three independent experiments (60 worms for each condition). UT: untreated worms. Statistical analysis was performed by one-way ANOVA with the Bonferroni post-test; asterisks indicate significant differences (*$p < 0.05$). C) Kaplan-Meier survival plot of *skn-1* mutant worms supplemented with 10 mM 2-HIBA. Lifespans of HGD untreated worms (UT) were reported as controls; n = 60 for each data point of single experiments (ns: not significant).

Since HGD also influences fatty acid metabolism, the effect of 2-HIBA on the accumulation of lipid reserves in *C. elegans* was evaluated by using the BODIPY fluorescent dye. In the presence of glucose, BODIPY staining detected large amounts of intestinal fat in untreated worms. Notably, 2-HIBA administration reduced that fat amount in a dose-dependent manner. In particular, histograms representing the percentage of lipid droplets highlighted a reduction of 30%, 50% and about 80% in worms treated with 5, 10 and 20 mM, respectively, as compared to control (Figure 19).

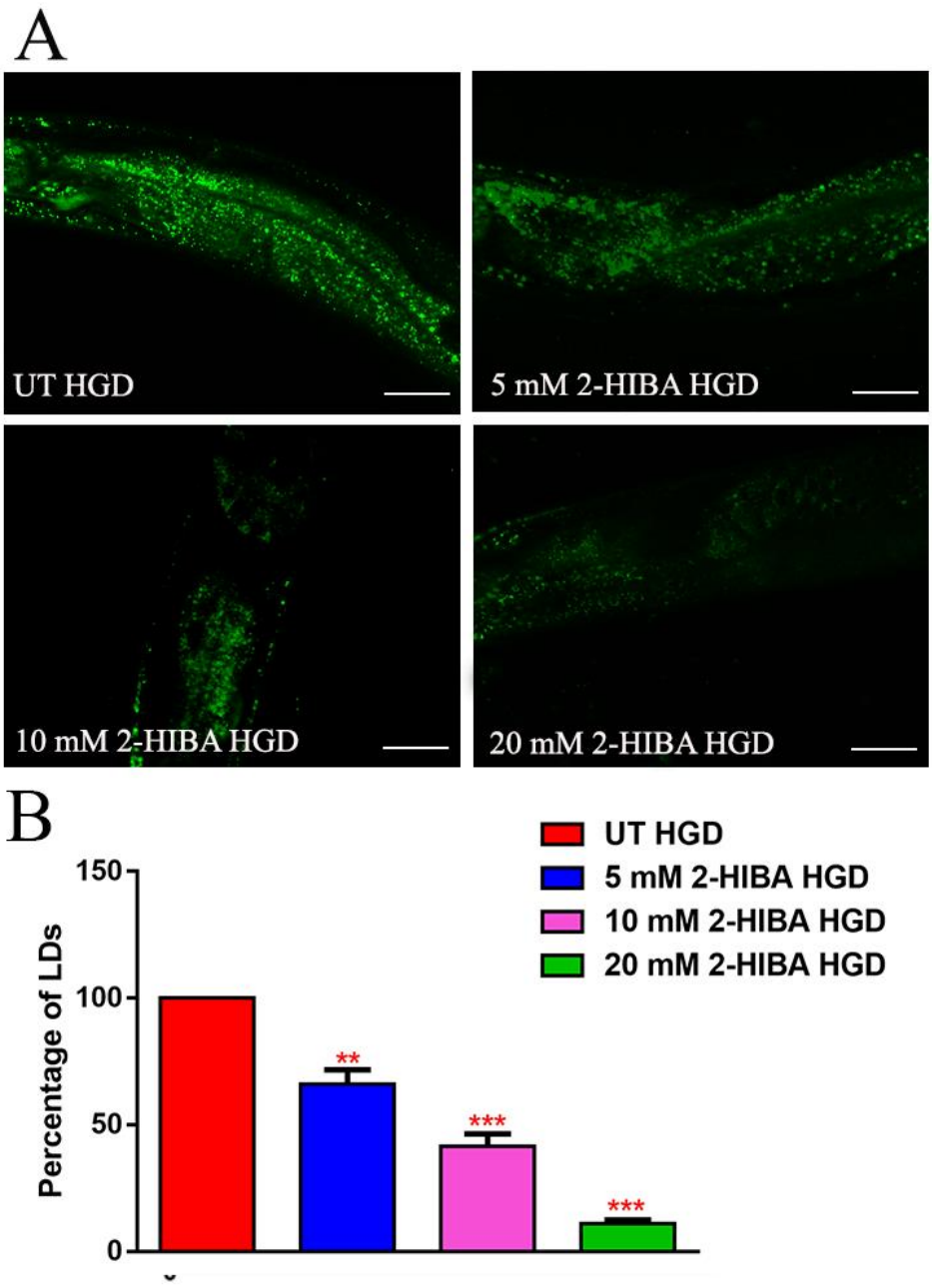

Figure 19. Lipid droplets accumulate in HGD worms. (A) BODIPY staining and (B) lipid droplets quantification in 1 day adult worms grown in the presence of glucose and fed with *E. coli* OP50 alone (UT: untreated) or supplemented with different 2-HIBA concentrations (** $p < 0.01$, ***$p < 0.001$). Scale bar = 50 μm

Results were confirmed by Coherent Anti-Stokes Raman Scattering (CARS) analysis (Figure 20). CARS microscopy consists in a label-free chemical imaging technique, allowing direct visualization of lipid-rich organelles due to the abundance of the CH_2 group. In agreement with BODIPY visualization, CARS images and fluorescence quantification showed that animals grown with HGD and supplemented with 2-HIBA revealed a proportional decrease in the accumulation of lipid droplets, as compared to the untreated population. Notably, among different concentrations, 10 mM 2-HIBA was able to significantly reduce lipofuscin auto-fluorescence, as highlighted by two photon fluorescence images (Figure 20).

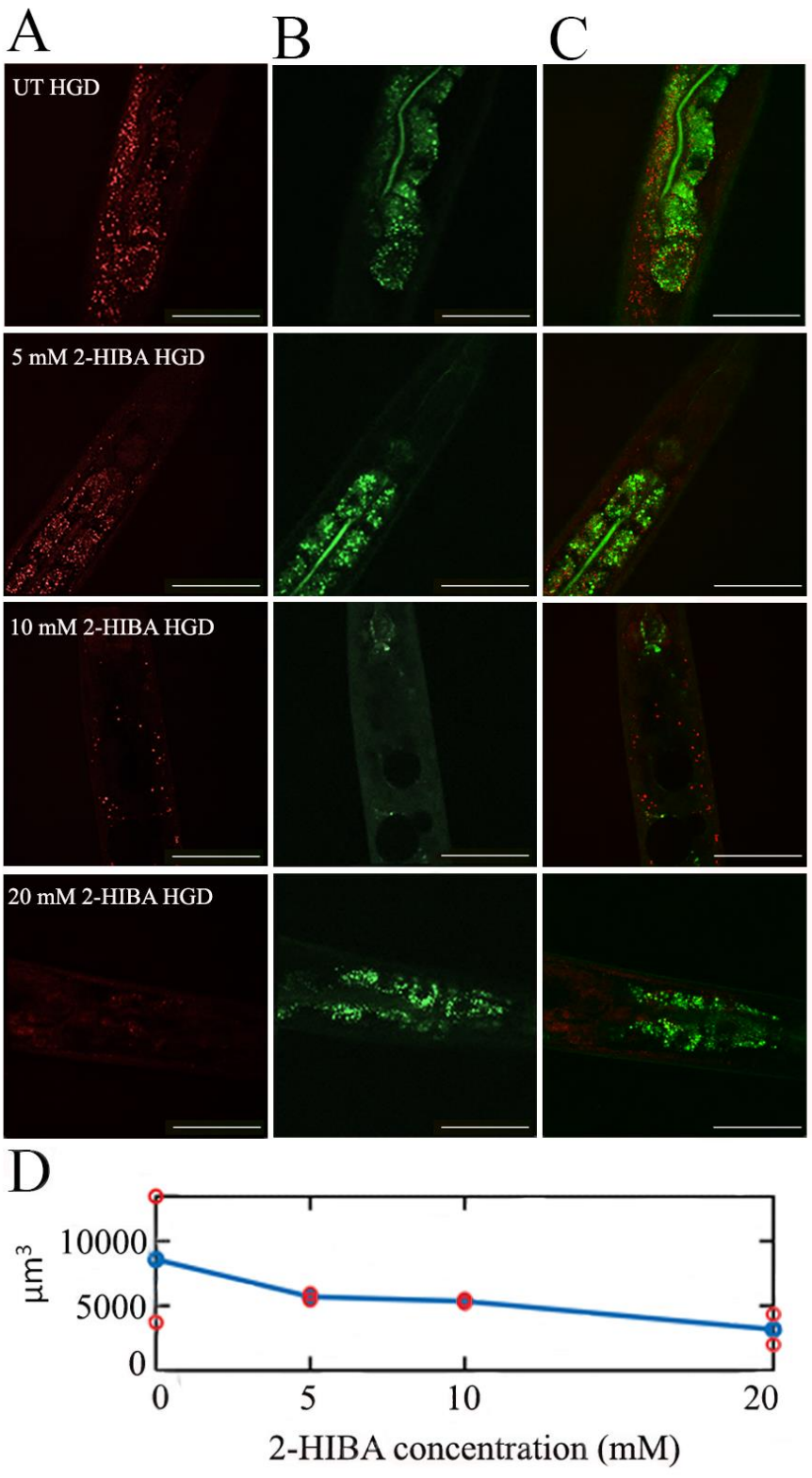

Figure 20. CARS microscopy of HGD worms treated with 2-HIBA at different concentrations. (A) CARS signals of lipid droplets and (B) two-photon auto-fluorescence image in early intestine and hypodermal cells in 1 day adult HGD worms treated or not with different concentrations of 2-HIBA, collected in the same region though our two-channel system. The combined image is reported in (C). The scale bar = 50 µm. (D) The lipid volume, detected in the CARS 3D stacks of images (two for each concentration), was reported by red circles, while the average was shown with blue circles.

Based on this set of results, also subsequent experiments were performed using 10 mM 2-HIBA. Interestingly, in HGD worms treated with 2-HIBA was observed a higher expression of *acs-2* (involved in β-oxidation), although there was an increase in the expression of genes involved in lipid synthesis (Figure 21A). In particular, animals supplemented with 10 mM 2-HIBA presented an increased transcription of about 70% for *sams-1*, and 1.5-fold increase for *fat-7* and *acs-2* genes, with the respect to the untreated control, while variations in *sbp-1* expression were not significant. Notably, comparing untreated nematodes grown with or without glucose, in HGD worms a significant 2.5-fold increase in *sbp-1* expression and a 50% reduction in *fat-7* transcript levels were observed (Figure 21B).

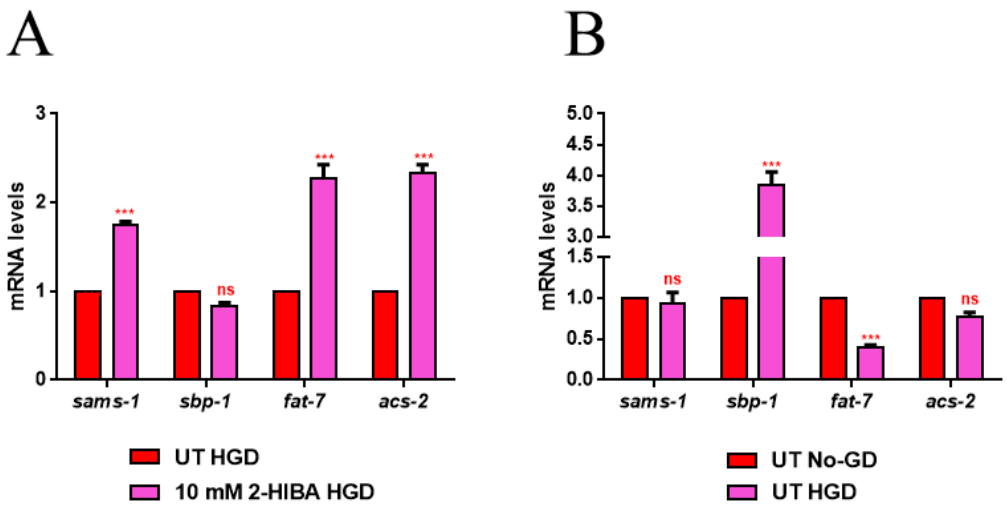

Figure 21. RT-qPCR analysis of lipid metabolism genes in HGD worms. (A) Expression of *sams-1*, *sbp-1*, *fat-7*, and *acs-2* genes in 2-HIBA HGD 1-day adults, compared to HGD untreated nematodes. (B) Expression of lipid metabolism genes in untreated populations, grown with (HGD) or without (No-GD) glucose. Experiments were performed in triplicate. Data are presented as mean ± SD (***p <0.001, ns: not significant).

Our results showed that treatment of 2-HIBA in HGD wild-type worms was able to extend lifespan, reduce aging and fat accumulation. In order to understand the possible involvement of *pep-2* gene in lifespan extension also in HGD condition, another set of experiment was performed on *pep-2* mutants. As shown in Figure 22, the treatment of 10 mM 2-HIBA in HGD *pep-2* mutants led to an effect on lifespan similar to that observed on untreated nematodes. Indeed, the median survival of mutant worms treated with 2-HIBA was recorded at day 8 in comparison with day 7 recorded in control mutants. Overall, these data confirm the requirement of *pep-2* for the 2-HIBA-dependent extension of lifespan.

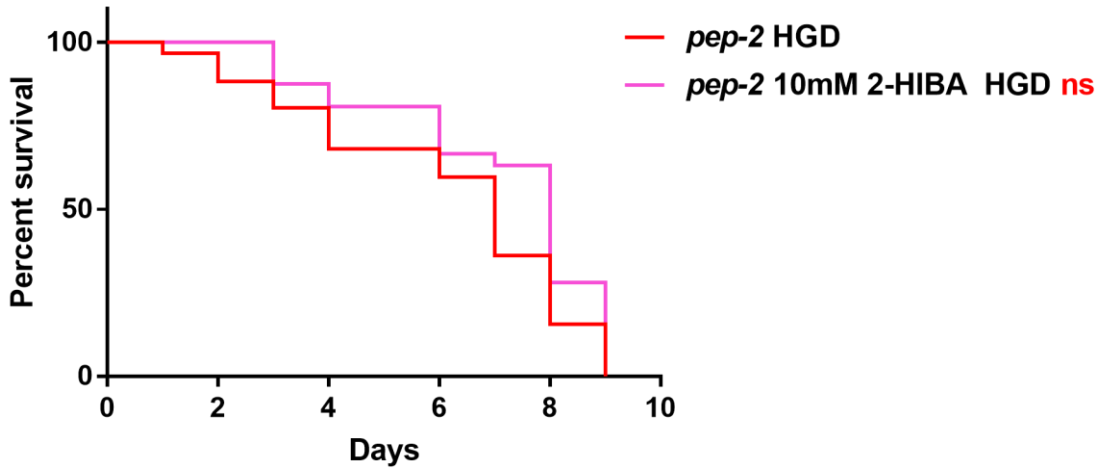

Figure 22. Effect of 2-HIBA on HGD *pep-2* mutant viability. Kaplan-Meier survival plot of HGD *pep-2* mutant worms supplemented or not with 10 mM 2-HIBA. n = 60 for each data point of single experiments (ns: not significant).

Moreover, fat accumulation in 10 mM 2-HIBA-fed *pep-2* mutants in the presence of glucose was about 20% lower than those detected in control population (Figure 23A and B). To identify the genes possibly responsible for the differences in fat storage induced by 10 mM 2-HIBA, a real-time qPCR analysis was performed in *pep-2* mutants (Figure 23C). Nematodes showed a significant increase of *acs-2* (involved in β-oxidation) mRNA levels when treated with 2-HIBA, while variations in *sams-1, sbp-1, fat-7* expression levels were not significant. Indeed, *pep-2* mutants supplemented with 10 mM 2-HIBA revealed an increased transcription of about two fold higher for *acs-2*, as compared to untreated worms. Interestingly, comparing nematodes treated with 2-HIBA grown with or without glucose, in HGD worms were observed a significant reduction of about 80% in *sams-1* and four-fold reduction in *sbp-1* and *fat-7* expression and a 50% increase in *acs-2* transcript levels (Figure 23C). These data suggest that the role of 2-HIBA in modulating lipid metabolism depends on diet, so further studies are needed to understand the pathway involved.

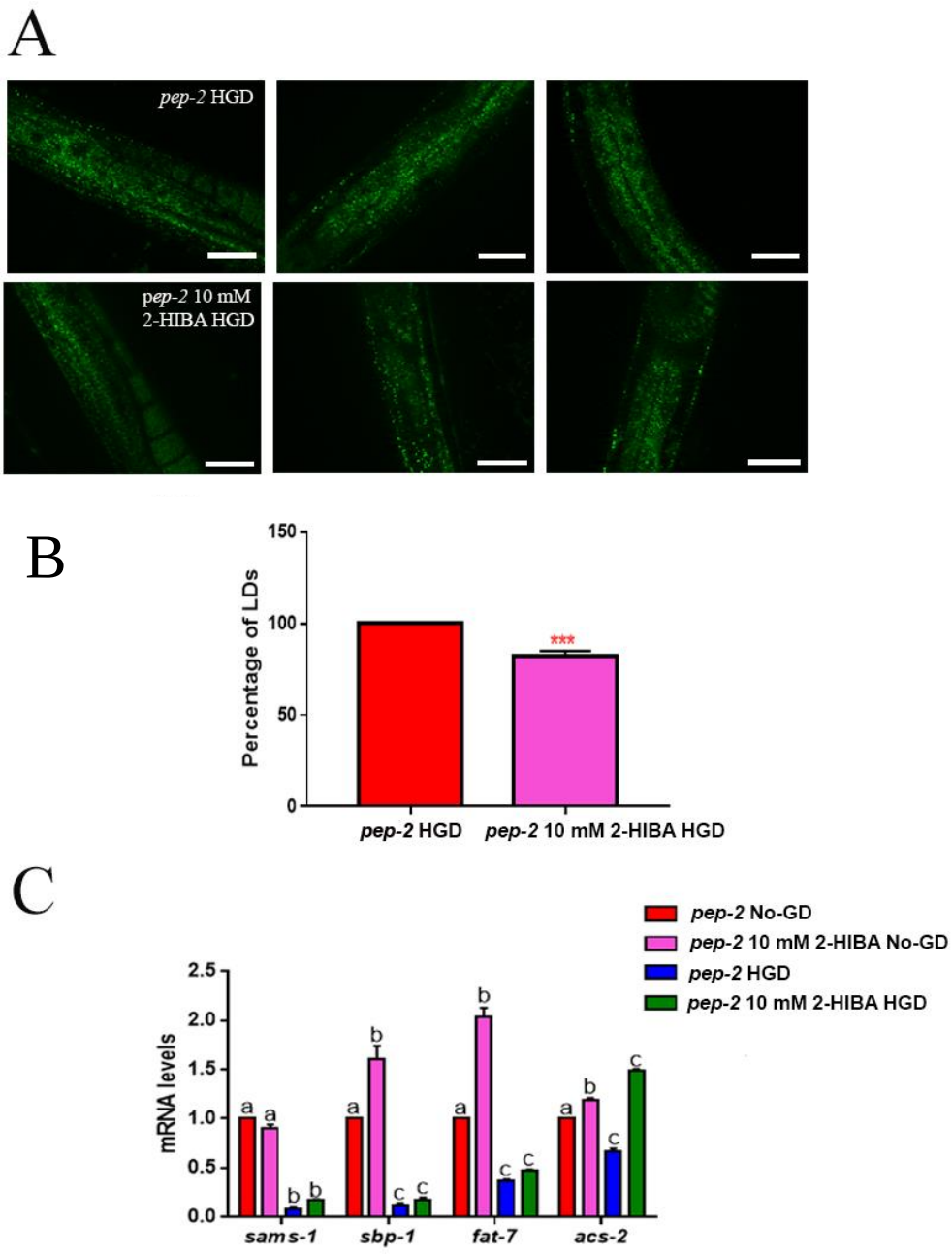

Figure 23. Fat accumulation in HGD *pep*-2 mutants.(A) BODIPY staining of 1-day adult *pep-2* mutant worms treated or not with 10 mM 2-HIBA supplemented with glucose Scale bar = 50 μm (B) Median Fluorescence Intensity (MFI) of fat accumulation observed by BODIPY staining. Statistical analysis was evaluated by one-way ANOVA with the Bonferroni post-test; asterisks indicate significant differences (***$p < 0.001$). Bars represent the mean of three independent experiments. (C) Expression of *sams-1*, *sbp-1*, *fat-7*, and *acs-2* genes in 10 mM 2-HIBA-fed 1 day adults *pep-2* mutants grown with (HGD) or without (No-GD) glucose. Histograms show the transcript levels of genes involved in lipid metabolism supplemented with 10 mM 2-HIBA HGD (green), 10 mM 2-HIBA No-GD (purple), *pep-2* untreated HGD (blue) as compared to untreated control No-GD (red). Experiments were performed in triplicate. Different letters indicate statistically significant differences ($p < 0.05$).

Metabolomics analysis

By ^{1}H-NMR metabolomics, a total of 43 metabolites, belonging to the classes of amino acids, fatty acids (FA), short chain fatty acids (SCFA), organic acids, glycerols, nitrogen compounds, nucleosides, carbohydrates, were identified and quantified (Supplementary Table S2). Comparing all the categories analysed, only quantitative, but no qualitative differences were observed. Representative hydroalcoholic and chloroformic ^{1}H-NMR profiles are shown in the supplementary material (Supplementary Figures S2, S3). The PLS-DA was performed on the controls matrix showed R^2 = 0.98 and Q^2 = 0.79 for the discrimination of nematodes grown on a glucose substrate (HGD) from those who grew without it (No-GD). The HGD group showed higher levels of betaine, glycine (Gly), adenosine-X-phosphate (AXP) and lower levels of monoacylglycerols (MAG), N-acetyl- moieties, lactate, tyrosine (Tyr), tryptophan (Trp), formate and U03 than No-GD. Univariate analysis, performed on each of these significant variables confirmed the statistical significance of MAG, Gly, Trp and AXP between the HGD and No-GD groups.

In order to observe the effect of HGD on 2-HIBA treated worms, a further PLS-DA analysis was performed on the fold-ratio matrix (paired 2-HIBA/untreated samples) on a reduced space of variables. The classification model showed R^2 = 0.86 and Q^2 = 0.51 and higher levels of Trp in the 2-HIBA-treated HGD group and were also statistically significant at the univariate analysis. The HGD group treated with 2-HIBA showed a 2.5 fold change as compared to the untreated.

It is known that TDO-2 plays a critical role in tryptophan metabolism by catalysing the first and rate-limiting step of the kynurenine pathway (Ren and Correira, 2000). In order to understand the possible effect induced by 2-HIBA on *tdo-2* gene, a real time q-PCR was performed. Worms treated with 2-HIBA in HGD conditions showed a transcriptional reduction of tdo-2 of about 50% as compared to control population (Figure 24).

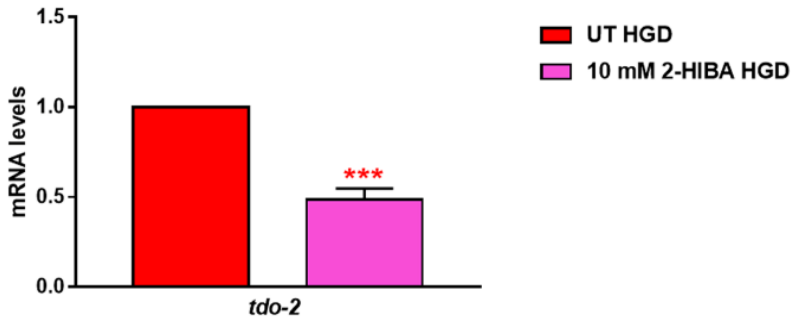

Figure 24. RT-qPCR analysis of *tdo2* gene in HGD worms. Expression of *tdo-2* gene in N2 worms in HGD condition treated with 10mM 2-HIBA (pink bars) and in untreated nematodes (red bars) at day 1 of adulthood. Experiments were performed in triplicate. Data are presented as mean ± SD (***p <0.001).

Discussion

The effects of 2-HIBA on *C. elegans* grown in standard conditions

In the present work, we took advantage of the simplified model organism *C. elegans* to evaluate the effect of 2-hydroxyisobutyric acid (2-HIBA), a cellular short-chain fatty acid (SCFA) isolated from urine of obese patients, on worm physiology. In the past years, molecular mechanisms involved in the aging process have been studied, since aging is one of the main risk factors for several chronic diseases such as type 2 diabetes and cancer (Hodes et al., 2016). Among the different concentrations tested on *C. elegans*, 10 mM 2-HIBA was found particularly effective to extend the lifespan, to delay ageing processes and to stimulate the oxidative stress responses in wild type nematodes. The pro-longevity effects observed in lifespan experiments were in agreement with the work of Edwards et al. (2014) on the ability of a HIB-like molecule, β-hydroxybutyrate, to increase the lifespan of *C. elegans*. Microscopy analysis demonstrated that 2-HIBA did not affect larval development, but it reduced fertility, possibly because nematodes spent more energy to survive and to contrast the ageing processes rather than to produce progeny, consistently with a previous work (Lee et al., 2015b). As compared to the untreated worms, the pumping rate measured at the 11th day of adulthood was higher and lipofuscin granules were reduced. Indeed, pumping rate consists in the number of contractions of the nematode's grinder, normally decreasing with ageing, while auto-fluorescence granules of lipofuscin accumulate along the old worm intestinal tissues (Papaevgeniou et al., 2017; Huang et al., 2004). These results suggested a pro-longevity effect of 2-HIBA linked to a delay of ageing processes in *C. elegans*.

Reactive oxygen species (ROS) are accumulated in organisms during ageing, generating an impairment that normally correlates with cellular damages and a diminished lifespan (Moreno-Arriola et al., 2014). Interestingly, in 2-HIBA treated worms we observed the activation of both p38 MAPK and IIS pathways and, therefore, a reduction of ROS levels.

The involvement of p38 MAPK pathways has been confirmed by the viability analysis performed on mutant animals depleted in genes encoding for SEK-1, PMK-1 or SKN-1 proteins, all belonging to the same MAPK signalling. The lifespan extension observed in wild-type worms was completely absent in these mutants supplemented with 2-HIBA. Migration of transcriptional factor SKN-1 into the nucleus was further corroborated by fluorescence microscopy.

The activation of the IIS pathway, that prevented DAF-16 from entering the nucleus and avoiding downstream *sod-3* and *gst-4* genes transcription, was confirmed by real-time q-PCR and fluorescence analysis. These observations confirmed the stimulation of 2-HIBA on both p38 MAPK and IIS pathways activation. Altogether, these results demonstrated that the effect of 2-HIBA on nematodes maintained the organisms' health and counteracted the adverse effects of ageing, through mechanisms of resistance to oxidative stress. Our data were consistent with previous studies that correlated pro-longevity and anti-ageing effects with a reduction of cellular stress (Miranda-Vizuete and Veal, 2017; Schifano et al., 2019). The increase of lipid droplet accumulation in 2-HIBA treated animals correlated with the activation of IIS pathway and the decrease in the

expression of *acs-2* gene, coding for a crucial enzyme involved in the fatty acid β-oxidation pathway (Coleman et al., 2002). These data, along with the enhanced expression of *sams-1*, *sbp-1* and *fat-7* genes involved in lipid biosynthesis, strengthen the evidence that the accumulation of fat storage in treated nematodes was probably due to an imbalance between synthesis and degradation of lipids. Among others, of particular interest was *fat-7* gene, which has been reported in maintaining appropriate levels of saturated and unsaturated fats in response to nutritional intake, inhibiting fatty acid β-oxidation and *acs-2* expression (Van Gilst et al., 2005).
To evaluate the role of 2-HIBA in obese worms, *pep-2* mutants were exploited. They lack intestinal di- and tri-peptide transporter that is involved in worm development and growth. Nematode mutants show an increase of body fat, resistance to oxidative stress, and a reduction in body size and progeny compared to N2 worms (Meissner et al., 2004; Spanier et al., 2009). Unlike wild type N2 strain, 10 mM 2-HIBA administration was not able to prolong life and to increase *sams-1* transcripts in *pep-2* worms. Moreover, regarding lipid accumulation, the slight increase of *acs-2* transcript levels, although significant, did not reach the high values observed for *fat-7* and *sbp-1* transcripts, emphasizing an additive effect of 2-HIBA on obese worms. These results were strongly linked to the increase of lipid accumulation observed with BODIPY staining.

The effects of 2-HIBA on *C. elegans* supplemented with a high-glucose diet

Glucose is an essential energy source for many cellular processes. The high-glucose diet (HGD) is related to obesity and pathological conditions and it is known to be linked to a higher production of ROS. Indeed, an altered glucose homeostasis negatively influenced the development, fertility and lifespan of organisms such as yeasts, worms, and mammals (Schulz et al., 2007; Edwards et al., 2015; Lee et al., 2015a; Alcántar-Fernández et al., 2018). Our results showed that reduced viability in HGD N2 worms was partially restored by 2-HIBA treatment, even if the median lifespan values did not reach the ones for worms grown in standard condition (No-GD). The metabolomic analysis highlighted a significant increase in tryptophan (Trp) levels in treated worms supplemented with HGD. The analysis of the transcript of *tdo2* gene, coding for an enzyme able to metabolize free Trp in the kynurenine pathway of Trp degradation, showed that *tdo2* gene expression is lower in 2-HIBA treated worms, as compared to untreated population; this suggested a down-regulated activity of degradation of Trp by 2-HIBA treatment. Indeed, previous studies reported that higher Trp levels were associated with depletion of tryptophan 2,3-dioxygenase (TDO) and lifespan extension in nematodes (van der Goot and Nollen, 2013; Edwards et al., 2015). Also, in HGD condition 2-HIBA was able to increase the pumping rate and reduce lipofuscin granules in old worms. Pro-longevity effects and the delay in aging in worms also depend on SKN-1 signaling (Edwards et al., 2015) and on the transcription factor DAF-16, which acts in the IIS pathway (van der Goot et al., 2012), therefore, the role of TDO might converge on some of these longevity factors. Previous data suggested that *daf-16* could be involved in lifespan regulation by *tdo-2* (van der Goot et al., 2012). Analysing *pep-2* mutant worms in HGD condition, 2-HIBA didn't have a positive effect to extend life span also suggesting the involvement of the *pep-2* gene in extending lifespan.

Unlike the No-GD conditions, microscopy analyses on HGD nematodes treated with different concentrations of 2-HIBA revealed a dose-dependent decrease of intestinal and hypodermal lipid droplets, in terms of distribution and morphology. Treatment with 10 mM 2-HIBA on HGD worms showed a further increment in the expression of *sams-1* and *fat-7* genes. However, in these nematodes also *acs-2* levels increased, unlike the reduction observed in No-GD treated animals. This could explain an enhancement in the β-oxidation process, compared to the untreated ones, resulting in a reduction of lipid vesicles. Our data showed that the 2-HIBA-dependent inverse relationship between *fat-7* and *acs-2* genes could be only observed in wild type nematodes grown in No-GD conditions, similarly to what was previously reported in conditions of starvation (Nomura et al., 2010). Conversely, in HGD conditions we observed a decrease of both *acs-2* and *fat-7* genes and a significant increase of the transcription of *sbp-1*. The caloric excess stimulates *sbp-1* expression in *C. elegans* as well as for SREBP-1c in mammals. Unexpectedly, for both obese *pep-2* model and HGD worms, we observed the increase in *acs-2* and *fat-7* genes, depending on 2-HIBA treatment. *fat-7* and *acs-2* expression is regulated by NHR-49 in response to short fasting through its interactions with SBP-1 (Nomura et al., 2010). NHR-49 is necessary for the expression of genes involved in fatty-acids-β-oxidation and lipid binding, while SBP-1 appeared to be involved in the expression of genes that participate in fatty acid synthesis. A possible relation between 2-HIBA and NHR-49 needs to be investigated.

Conclusion

In conclusion, 2 HIBA, a molecule isolated from the urine of obese subjects, unexpectedly induced positive effects on *C.elegans*. Overall, 2-HIBA treatment extended lifespan and induced anti-ageing effects, protecting against oxidative stress in *C. elegans*. These responses seem to occur through induction of insulin/IGF-1 signaling (IIS) and p38 MAPK pathways and are dependent on PEP-2 activation. In HGD conditions, the pro-longevity effect appeared to be correlated to higher levels of Trp, which might play a role in restoring the decreased viability observed in the HGD untreated nematodes. The effect of 2-HIBA on HGD worms resulted in a reduction of the lipid droplets deposition, accordingly with an increase of acs-2 and ech-1 genes transcription, involved in β-oxidation processes.

Based on what we observed in HGD condition, we inferred that the presence of 2-HIBA in human urines could be linked to counteracting the accumulation of lipids as a response to a diet characterized by a high carbohydrate content.

Materials and Methods

C. elegans strains and growth conditions

The *C. elegans* strains used were: wild-type N2, CL2166 (dvIs19 [(pAF15)gst-4p::GFP::NLS] III), CF1553 (*muls84[pAD76(Sod-3::GFP)]*), LD1 (ldIs7 [skn-1b/c::GFP + rol-6(su1006)] and TJ356 (zIs356 [daf-16p::daf-16a/b::GFP + rol-6(su1006)]) transgenic strains. Mutant strains used were KU25 *pmk-1*(km25), AU1 *sek-1*(ag-1), QV225 *skn-1*(zj15) and *pep-2* [*pept-1*(lg601)]. Nematodes were grown on nematode growth medium (NGM) and fed with heat killed *Escherichia coli* OP50 and 2-hydroxyisobutyric acid, 99% (Sigma-Aldrich) at different concentrations (5, 10 or 20 mM), as indicated. In detail, 60 μL of heat-killed OP50 culture was spread on 3.5 cm diameter NGM plates and 60 μL of 2-HIBA was added. Heat-killed OP50 cells were prepared as follows: bacteria were cultured overnight in LB broth at 37°C, centrifuged at 6000 rpm for 15 min and suspended in 2 mL of sterile water. Cells were then incubated at 65°C for 90 min and deposited onto NGM agar plates. Heat-killed cells were also plated on Luria-Bertani (LB) agar in parallel to ensure that no viable cells remained.

C. elegans lifespan assay

Fertile adults were placed to lay embryos for 8 h on NGM spread with *E. coli* OP50 and 2-HIBA at different concentrations and then sacrificed. All lifespan assays started when the progeny became fertile (t0). Nematodes grown on *E. coli* OP50 alone were taken as controls. Lifespan analysis was performed at 16°C and worms were daily transferred to new plates seeded with fresh lawns. They were scored as dead when they no longer responded to gentle touch with a platinum wire. At least 60 nematodes per condition were used in each experiment. To mimic high-glucose diets (HGD), 2% glucose (Sigma) was added to the mix of agar and salts of the NGM and experiments were performed at 20°C. Animals were transferred to new plates seeded with fresh lawns and monitored daily.

Brood size and body size analysis

Synchronized worms were incubated at 16°C on NGM plates seeded with of OP50 HK and 60 μl of 2-HIBA at different concentrations, allowing embryos to lay. Next, animals were transferred onto a fresh bacteria plate every day, and the number of progeny was counted with a Zeiss Axiovert 25 microscope. The procedure was repeated until the mother worms stopped laying eggs. Each day, the progeny production was recorded and was compared with the OP50 HK- or HIB-fed nematodes. For body size analysis, individual animals were photographed after 1, 2, 3, 4 and 5 days from egg hatching using a Leica MZ10F stereomicroscope connected to Jenoptik CCD camera. 2-HIBA-fed worm length was determined by using the Delta Sistemi IAS software and compared to OP50 HK fed worms. At least 30 nematodes were imaged on at least three independent experiments.

Pumping rate and lipofuscin analysis

About 10 worms for each condition were analyzed at the stage of young and old worms. Pumping rate was measured under Zeiss Axiovert 25 microscope by counting the number of grinder contractions of 10 animals for each treatment, during a period of 30 s. To analyze the auto-fluorescence of lipofuscin granules, 10 worms for each condition were washed three times with M9 buffer. Nematodes were then placed onto a 3% agar pad containing 20 mmol L^{-1} sodium azide and then observed by Zeiss Axiovert 25 microscope.

Body length measurements

Individual animals were photographed after 1, 2, 3, 4 and 5 days from egg hatching using a Leica MZ10F stereomicroscope connected to Jenoptik CCD camera. HIB-fed worms' length was determined by using the Delta Sistemi IAS software and compared to OP50 HK fed worms. At least 30 nematodes were imaged on at least three independent experiments.

Fluorescence analysis in the transgenic strains

At the stage of 1 day of adulthood, synchronized *gst-4*::GFP, *sod-3*::*GFP*, *daf-16*::GFP and *skn-1*::GFP transgenic worms fed heat killed OP50 and 10 mM 2-HIBA were anesthetized with sodium azide (20 mmol L^{-1}) and observed under a Zeiss Axiovert 25 microscope. The experiments were repeated three times and 15 worms per group were used in each experiment.

Evaluation of reactive oxygen species (ROS) levels

ROS formation in 1-day adult worms was measured using the fluorescent probe H2DCFDA. After larval development on the different conditions, 1-day adult worms were collected (in triplicate) into 0.1 mL of M9, washed three times and 0.1 mL of 100 μM L^{-1} H_2DCF-DA (SIGMA-ALDRICH, Milan, Italy) in methanol was added in each sample, to obtain a final concentration of 50 μM. H_2DCF-DA is a membrane-permeable non-fluorescent probe, which can enter the cells of the worm and it is intracellularly converted to H_2DCFs. This probe can be oxidized by ROS to yield the fluorescent dye DCF. The changes of fluorescence in worms indicate the accumulation of ROS. After 4 hours of dark incubation at 20°C, worms were analysed by fluorescence microscopy (Zeiss Axiovert 25, Jena, Germany). MFI was analysed using ImageJ Software.

BODIPY staining

About 60 1-day adult nematodes, grown on OP50 HK supplemented or not with 10 mM 2-HIBA, were washed three times with M9 buffer. Worms were then incubated with a solution of 6.7 μg/mL BODIPY 493/503 (Life Technologies, Milan, Italy) for 20 min. Afterwards, nematodes were mounted onto 3% agarose pads containing 20 mM sodium azide and observed with Axio Observer Z1 inverted microscope, equipped with an ApoTome.2

System (Carl Zeiss Inc., Oberkochen, Germany). Digital images were acquired with the AxioCam MRm high-resolution digital camera (Zeiss) and processed with the AxioVision 4.8.2 software (Zeiss). ApoTome optical sectioning images of animals were recorded under 40 Å~/0.75 objective (Zeiss). Fluorescence mean was analysed using ImageJ software.

Coherent Anti-Stokes Raman Scattering and two-photon fluorescence microscopy

A 7 picosecond laser source (Levante Emerald OPO, APE Angewandte Physik & Elektronik GmbH, Germany, pumped by a Nd:Vanadate laser at 1064 nm, High Q Laser GmbH, Austria) generated two pulses at 76 MHz repetition rate, with powers of 70 mW and 120 mW for the pump (817 nm) and Stokes (1064 nm) beams, that were spatially and temporally overlapped and then coupled to a modified inverted laser scanning microscope with a couple of galvo mirrors. A 40×/NA = 1.3 objective (Olympus UPLFLN40X) was used to focus both beams. This setup is able to generate CARS signals, when the focal spot is rich in CH vibration at 2840 cm^{-1}, as in the case of lipids. The emitted CARS signal (at 663 nm) and the two-photon fluorescence (in the range of 495-540 nm), collected through the same objective (EPI direction), were detected with two photomultipliers (Yen et al., 2010). One day adult worms, treated or not with 2-HIBA, were placed in a droplet of Levamisole (1 mM) on a 0.17-mm-thick microscopy cover glass covered with a thin agarose film. A second cover glass was then gently applied on the sample.

A 3D stacks of images was performed with a step of 2 μm. The images were collected over a square field of 150.5 μm with a later pixel size of 0.147 μm (1024X1024 pixels). For the calculation of lipid droplets, the slow modulations (not related to the lipid droplets) were removed subtracting the same image after a gaussian blurring with standard deviation equal to 20 pixels. Then, the volume was calculated counting the pixels above a specific threshold (equal for each worm).

Real Time qPCR

At the stage of 1 day of adulthood, total RNA from 200 worms for each sample was isolated with RNeasy midi kit (Qiagen) according to manufacturer's instructions and then digested with 2 U/μL DNAse I (Ambion). One microgram of each sample was reverse-transcribed using oligo-dT and enhanced Avian reverse transcriptase (SIGMA, Cat. Number A4464), according to manufacturer's instructions. For real-time qPCR assay, each well contained 2 μL of cDNA used as template, SensiMix SYBR & Fluorescein Kit purchased from Bioline, and the selective primers (200 nM) for gene involved in fat accumulation and oxidative stress were reported in Table S1. I Cycler IQ Multicolor Real-Time Detection System (Biorad) was used for the analysis. The real-time PCR conditions included a denaturing step at 95 °C for 3 min followed by 40 cycles at 95 °C for 30 s, 55 °C for 30 s, and 75 °C for 45 s. Two cycles were included as final steps: one at 95 °C (1 min) and the other at the annealing temperature specific for each couple of primers used (1 min). Quantification was performed using a comparative C_T method (C_T = threshold cycle value). Briefly, the differences between the mean C_T value of

each sample and the C_T value of the housekeeping gene (*act-1*) were calculated: $\Delta C_{Tsample} = C_{Tsample} - C_{ACT1}$. Final result was determined as $2^{-\Delta\Delta CT}$ where $\Delta\Delta C_T = \Delta C_{Tsample} - \Delta C_{Tcontrol}$. The experiment was performed in triplicate.

Sample preparation and NMR analysis

For the metabolomic analysis, 7 couples of *C. elegans*, made of 7 samples of nematodes fed OP50 and 7 samples of nematodes treated with 10 mM 2-HIBA, were compared to 10 couples of *C. elegans* grown on a highly glucose-enriched diet, made of 10 samples of nematodes fed OP50 and 10 samples of nematodes treated with 10mM 2-HIBA.

C. elegans extraction procedure. To about 3000 frozen worms stored in polypropylene tubes, 1mL of sterilized glass beads and 2 mL of iced MeOH were added. Nematodes were then subjected to 8 cycles of 2 minutes vortex and 2 minutes of rest in ice. The supernatant was picked up and the beads were washed with a mixture of 2 mL iced MeOH and 1 mL iced $CHCl_3$, then vortexed. The supernatant was added to the previous one and the beads were again washed in 3 mL of iced $CHCl_3$ and then vortexed. The final supernatant was added to the previous pool. Finally, 2 mL of H_2O were added to the beads for washing, subsequently vortexed and the supernatant was added to the pool. Samples were kept overnight at 4°C. After the centrifugation at 10,000 × *g* at 4°C for 25 minutes, the hydroalcoholic and the chloroformic phases were separately collected, dried under N_2 stream and preserved at −80°C until the subsequent analysis. Each dried polar sample was suspended in 700 µl of D_2O containing 3-(trimethylsilyl)-propionic-2,2,3,3-D_4 acid sodium salt (final concentration of TSP: 2 mM) (Sigma-Aldrich, St. Louis, MO, United States), as an internal chemical shift and concentration standard. The organic phase was resuspended in 700 µl of $CDCl_3$ with hexamethyldisiloxane (final concentration of HMDS: 2 mM) (Sigma-Aldrich, St. Louis, MO, United States) as an internal standard.

NMR analysis. Five mm NMR glass tubes were used for the NMR analysis. All spectra were recorded at 298 K on a high resolution JEOL 600 MHz spectrometer (JEOL Ltd, Akishima, Japan) equipped with cryo-probe. To univocally identify the metabolites in the biological samples, bidimensional experiments ^{1}H-^{1}H TOCSY (TOtal Correlation SpectroscopY) and ^{1}H-^{13}C HSQC (Heteronuclear Single Quantum Correlation) were performed on selected samples. Identification was confirmed by comparison with literature (Geier et al., 2011; Zanni et al., 2017), web database (Wishart et al., 2012) and in-house databases.

Mono-dimensional NMR spectra were processed and quantified by using ACD/Lab 1D NMR Manager ver. 12.0 software (Advanced Chemistry Development, Inc., Toronto, ON, Canada), whereas bi-dimensional NMR spectra were processed by using Delta NMR Software v 5.3.1 (JEOL Ltd, Akishima, Japan) and MestreNova v 11.0 (Mestrelab Research SL, Santiago de Compostela, Spain). Metabolites' quantification was carried out by comparing the integrals of specific metabolites resonances with the one of their specific internal standards.

Statistical analysis

The statistical significance was perfomed by Student's t-test or one-way ANOVA analysis coupled with a Bonferroni post-test (GraphPad Prism 5.0 software, GraphPad Software Inc., La Jolla, CA, USA). Differences with p values < 0.05 were considered significant and were indicated as follows: $^{*}p < 0.05$, $^{**}p < 0.01$, and $^{***}p < 0.001$. Experiments were performed at least in triplicate. Data were presented as mean ± SD. For fluorescence images, median fluorescence intensity was analyzed using the ImageJ software, measuring the ratio of pixels per area of the worm.

References

Alcántar-Fernández, J., Navarro, R. E., Salazar-Martínez, A. M., Pérez-Andrade, M. E., and Miranda-Ríos, J. (2018). Caenorhabditis elegans respond to high-glucose diets through a network of stress-responsive transcription factors. *PLoS ONE* 13, e0199888. doi: 10.1371/journal.pone.0199888.

Amin, A. M. (2021). "Metabolomics applications in coronary artery disease personalized medicine," in *Advances in Clinical Chemistry* (Elsevier), 233–270. doi: 10.1016/bs.acc.2020.08.003.

Arneth, B., Arneth, R., and Shams, M. (2019). Metabolomics of Type 1 and Type 2 Diabetes. *IJMS* 20, 2467. doi: 10.3390/ijms20102467.

Baumeister, R., Schaffitzel, E., and Hertweck, M. (2006). Endocrine signaling in Caenorhabditis elegans controls stress response and longevity. *Journal of Endocrinology* 190, 191–202. doi: 10.1677/joe.1.06856.

Calvani, R., Miccheli, A., Capuani, G., Tomassini, A., Puccetti, C., Delfini, M., et al. (2010). Gut microbiome-derived metabolites characterize a peculiar obese urinary metabotype. *Int J Obes* 34, 1095–1098. doi: 10.1038/ijo.2010.44.

Coleman, R. A., Lewin, T. M., Van Horn, C. G., and Gonzalez-Baró, M. R. (2002). Do Long-Chain Acyl-CoA Synthetases Regulate Fatty Acid Entry into Synthetic Versus Degradative Pathways? *The Journal of Nutrition* 132, 2123–2126. doi: 10.1093/jn/132.8.2123.

Dai, L., Peng, C., Montellier, E., Lu, Z., Chen, Y., Ishii, H., et al. (2014). Lysine 2-hydroxyisobutyrylation is a widely distributed active histone mark. *Nat Chem Biol* 10, 365–370. doi: 10.1038/nchembio.1497.

Diaz, S. O., Pinto, J., Graça, G., Duarte, I. F., Barros, A. S., Galhano, E., et al. (2011). Metabolic Biomarkers of Prenatal Disorders: An Exploratory NMR Metabonomics Study of Second Trimester Maternal Urine and Blood Plasma. *J. Proteome Res.* 10, 3732–3742. doi: 10.1021/pr200352m.

Dong, H., Guo, Z., Feng, W., Zhang, T., Zhai, G., Palusiak, A., et al. (2018). Systematic Identification of Lysine 2-hydroxyisobutyrylated Proteins in Proteus mirabilis. *Molecular & Cellular Proteomics* 17, 482–494. doi: 10.1074/mcp.RA117.000430.

Edwards C, Copes N, Bradshaw PC. D-ß-hydroxybutyrate: an anti-aging ketone body. *Oncotarget*. 2014;6(6):3477-3478. doi:10.18632/oncotarget.3423

Edwards, C., Canfield, J., Copes, N., Brito, A., Rehan, M., Lipps, D., et al. (2015). Mechanisms of amino acid-mediated lifespan extension in Caenorhabditis elegans. *BMC Genet* 16, 8. doi: 10.1186/s12863-015-0167-2.

Ehmke, M., Luthe, K., Schnabel, R., & Döring, F. (2014). S-Adenosyl methionine synthetase 1 limits fat storage in Caenorhabditis elegans. *Genes & nutrition*, *9*(2), 386. https://doi.org/10.1007/s12263-014-0386-6

Elliott, P., Posma, J. M., Chan, Q., Garcia-Perez, I., Wijeyesekera, A., Bictash, M., et al. (2015). Urinary metabolic signatures of human adiposity. *Sci. Transl. Med.* 7. doi: 10.1126/scitranslmed.aaa5680.

Flier JS (2004). Obesity wars: molecular progress confronts an expanding epidemic. Cell Press Jan 23;116(2):337-50. doi: 10.1016/s0092-8674(03)01081-x.

Friedrich, N., Budde, K., Wolf, T., Jungnickel, A., Grotevendt, A., Dreßler, M., et al. (2012). Short-Term Changes of the Urine Metabolome After Bariatric Surgery. *OMICS: A Journal of Integrative Biology* 16, 612–620. doi: 10.1089/omi.2012.0066.

Gasmi, A., Mujawdiya, P. K., Noor, S., Piscopo, S., & Menzel, A. (2021). Lifestyle Genetics-Based Reports in the Treatment of Obesity. *Archives of Razi Institute*, *76*(4), 707–719. https://doi.org/10.22092/ari.2021.356057.1768

Geier, F. M., Want, E. J., Leroi, A. M., and Bundy, J. G. (2011). Cross-Platform Comparison of *Caenorhabditis elegans* Tissue Extraction Strategies for Comprehensive Metabolome Coverage. *Anal. Chem.* 83, 3730–3736. doi: 10.1021/ac2001109.

Giglio MP, Hunter T, Bannister JV, Bannister WH, Hunter GJ. (1994) The manganese superoxide dismutase gene of Caenorhabditis elegans. Biochem Mol Biol Int. May;33(1):37-40. PMID: 8081211.

Gil, A. M., Duarte, D., Pinto, J., and Barros, A. S. (2018). Assessing Exposome Effects on Pregnancy through Urine Metabolomics of a Portuguese (Estarreja) Cohort. *J. Proteome Res.* 17, 1278–1289. doi: 10.1021/acs.jproteome.7b00878.

Guerra, J. V. S., Dias, M. M. G., Brilhante, A. J. V. C., Terra, M. F., García-Arévalo, M., and Figueira, A. C. M. (2021). Multifactorial Basis and Therapeutic Strategies in Metabolism-Related Diseases. *Nutrients* 13, 2830. doi: 10.3390/nu13082830.

Hodes RJ, Sierra F, Austad SN, Epel E, Neigh GN, Erlandson KM, Schafer MJ, LeBrasseur NK, Wiley C, Campisi J, Sehl ME, Scalia R, Eguchi S, Kasinath BS, Halter JB, Cohen HJ, Demark-Wahnefried W, Ahles TA, Barzilai N, Hurria A, Hunt PW. (2016) Disease drivers of aging. Ann N Y Acad Sci. Dec;1386(1):45-68. doi: 10.1111/nyas.13299.

Houstis N, Rosen ED, Lander ES. (2006) Reactive oxygen species have a causal role in multiple forms of insulin resistance. Nature. Apr 13;440(7086):944-8. doi: 10.1038/nature04634.

Huang, C., Xiong, C., and Kornfeld, K. (2004). Measurements of age-related changes of physiological processes that predict lifespan of *Caenorhabditis elegans*. *Proc. Natl. Acad. Sci. U.S.A.* 101, 8084–8089. doi: 10.1073/pnas.0400848101.

Huang, H., Luo, Z., Qi, S., Huang, J., Xu, P., Wang, X., et al. (2018a). Landscape of the regulatory elements for lysine 2-hydroxyisobutyrylation pathway. *Cell Res* 28, 111–125. doi: 10.1038/cr.2017.149.

Huang, H., Tang, S., Ji, M., Tang, Z., Shimada, M., Liu, X., et al. (2018b). p300-Mediated Lysine 2-Hydroxyisobutyrylation Regulates Glycolysis. *Molecular Cell* 70, 663-678.e6. doi: 10.1016/j.molcel.2018.04.011.

Huang, J., Luo, Z., Ying, W., Cao, Q., Huang, H., Dong, J., et al. (2017). 2-Hydroxyisobutyrylation on histone H4K8 is regulated by glucose homeostasis in *Saccharomyces cerevisiae*. *Proc. Natl. Acad. Sci. U.S.A.* 114, 8782–8787. doi: 10.1073/pnas.1700796114.

Inoue H, Hisamoto N, An JH, Oliveira RP,Nishida E, Blackwell TK, Matsumoto K (2005). The C. elegans p38 MAPK pathway regulates nuclear localization of the transcription factor SKN-1 in oxidative stress response. *Genes Dev.* 19(19):2278-83. doi: 10.1101/gad.1324805.

Irwin, C., Mienie, L. J., Wevers, R. A., Mason, S., Westerhuis, J. A., van Reenen, M., et al. (2018). GC–MS-based urinary organic acid profiling reveals multiple dysregulated metabolic pathways following experimental acute alcohol consumption. *Sci Rep* 8, 5775. doi: 10.1038/s41598-018-24128-1.

Karlsson FH, Tremaroli V, Nookaew I, Bergström G, Behre CJ, Fagerberg B, Nielsen J, Bäckhed F. (2013) Gut metagenome in European women with normal, impaired and diabetic glucose control. Nature. Jun 6;498(7452):99-103. doi: 10.1038/nature12198.

Lee, D., Jeong, D.-E., Son, H. G., Yamaoka, Y., Kim, H., Seo, K., et al. (2015a). SREBP and MDT-15 protect *C. elegans* from glucose-induced accelerated ageing by preventing accumulation of saturated fat. *Genes Dev.* 29, 2490–2503. doi: 10.1101/gad.266304.115.

Lee, J., Kwon, G., and Lim, Y.-H. (2015b). Elucidating the Mechanism of Weissella-dependent Lifespan Extension in Caenorhabditis elegans. *Sci Rep* 5, 17128. doi: 10.1038/srep17128.

Li, M., Wang, B., Zhang, M., Rantalainen, M., Wang, S., Zhou, H., et al. (2008). Symbiotic gut microbes modulate human metabolic phenotypes. *Proc. Natl. Acad. Sci. U.S.A.* 105, 2117–2122. doi: 10.1073/pnas.0712038105.

Li, Y., Xu, J., and Su, X. (2017). Analysis of Urine Composition in Type II Diabetic Mice after Intervention Therapy Using Holothurian Polypeptides. *Front. Chem.* 5, 54. doi: 10.3389/fchem.2017.00054.

Lynch, C. J., & Adams, S. H. (2014). Branched-chain amino acids in metabolic signalling and insulin resistance. *Nature reviews. Endocrinology*, *10*(12), 723–736. https://doi.org/10.1038/nrendo.2014.171

Magne, F., Gotteland, M., Gauthier, L., Zazueta, A., Pesoa, S., Navarrete, P., & Balamurugan, R. (2020). The Firmicutes/Bacteroidetes Ratio: A Relevant Marker of Gut Dysbiosis in Obese Patients?. *Nutrients*, *12*(5), 1474. https://doi.org/10.3390/nu12051474

Markaki, M., and Tavernarakis, N. (2010). Modeling human diseases in Caenorhabditis elegans. *Biotechnology Journal* 5, 1261–1276. doi: 10.1002/biot.201000183.

Marrocco, F., Delli Carpini, M., Garofalo, S. *et al.* Short-chain fatty acids promote the effect of environmental signals on the gut microbiome and metabolome in mice. *Commun Biol* **5**, 517 (2022). https://doi.org/10.1038/s42003-022-03468-9.

McMurray F, Patten DA, Harper ME. (2016) Reactive Oxygen Species and Oxidative Stress in Obesity-Recent Findings and Empirical Approaches. Obesity (Silver Spring). Nov;24(11):2301-2310. doi: 10.1002/oby.21654.

Meissner, B., Boll, M., Daniel, H., and Baumeister, R. (2004). Deletion of the Intestinal Peptide Transporter Affects Insulin and TOR Signaling in Caenorhabditis elegans. *Journal of Biological Chemistry* 279, 36739–36745. doi: 10.1074/jbc.M403415200.

Mi, K., Jiang, Y., Chen, J., Lv, D., Qian, Z., Sun, H., et al. (2020). Construction and Analysis of Human Diseases and Metabolites Network. *Front. Bioeng. Biotechnol.* 8, 398. doi: 10.3389/fbioe.2020.00398.

Miccheli, A., Capuani, G., Marini, F., Tomassini, A., Praticò, G., Ceccarelli, S., et al. (2015). Urinary 1H-NMR-based metabolic profiling of children with NAFLD undergoing VSL#3 treatment. *Int J Obes* 39, 1118–1125. doi: 10.1038/ijo.2015.40.

Miranda-Vizuete, A., and Veal, E. A. (2017). Caenorhabditis elegans as a model for understanding ROS function in physiology and disease. *Redox Biology* 11, 708–714. doi: 10.1016/j.redox.2016.12.020.

Moreno-Arriola, E., Cárdenas-Rodríguez, N., Coballase-Urrutia, E., Pedraza-Chaverri, J., Carmona-Aparicio, L., and Ortega-Cuellar, D. (2014). *Caenorhabditis elegans* : A Useful Model for Studying Metabolic Disorders in Which Oxidative Stress Is a Contributing Factor. *Oxidative Medicine and Cellular Longevity* 2014, 1–9. doi: 10.1155/2014/705253.

Morrison, D. J., & Preston, T. (2016). Formation of short chain fatty acids by the gut microbiota and their impact on human metabolism. *Gut microbes*, *7*(3), 189–200. https://doi.org/10.1080/19490976.2015.1134082

Nakagawa H, Shiozaki T, Kobatake E, Hosoya T, Moriya T, Sakai F, Taru H, Miyazaki T. (2016). Effects and mechanisms of prolongevity induced by Lactobacillus gasseri SBT2055 in Caenorhabditis elegans. *Aging Cell.* Apr;15(2):227-36. doi: 10.1111/acel.12431.

Newgard, C. B. (2012). Interplay between Lipids and Branched-Chain Amino Acids in Development of Insulin Resistance. *Cell Metabolism* 15, 606–614. doi: 10.1016/j.cmet.2012.01.024.

Nicholson JK, Holmes E, Kinross J, Burcelin R, Gibson G, Jia W, Pettersson S. (2012). Host-gut microbiota metabolic interactions. Science 336: 1262–1267. doi: 10.1126/science.1223813.

Nie C, He T, Zhang W, Zhang G, Ma X. (2018). Branched Chain Amino Acids: Beyond Nutrition Metabolism. *International Journal of Molecular Sciences*; 19(4):954. https://doi.org/10.3390/ijms19040954

Nomura, T., Horikawa, M., Shimamura, S., Hashimoto, T., and Sakamoto, K. (2010). Fat accumulation in Caenorhabditis elegans is mediated by SREBP homolog SBP-1. *Genes Nutr* 5, 17–27. doi: 10.1007/s12263-009-0157-y.

Papaevgeniou, N., Hoehn, A., Grune, T., and Chondrogianni, N. (2017). Lipofuscin effects in Caenorhabditis elegans ageing model. *Free Radical Biology and Medicine* 108, S48. doi: 10.1016/j.freeradbiomed.2017.04.175.

Parada Venegas, D., De la Fuente, M. K., Landskron, G., González, M. J., Quera, R., Dijkstra, G., Harmsen, H. J. M., Faber, K. N., & Hermoso, M. A. (2019). Short Chain Fatty Acids (SCFAs)-Mediated Gut Epithelial and Immune Regulation and Its Relevance for Inflammatory Bowel Diseases. *Frontiers in immunology*, *10*, 277. https://doi.org/10.3389/fimmu.2019.00277

Pi-Sunyer X. (2009). The medical risks of obesity. Postgraduate medicine, 121(6), 21–33. doi: 10.3810/pgm.2009.11.2074.

Porez, G., Prawitt, J., Gross, B., and Staels, B. (2012). Bile acid receptors as targets for the treatment of dyslipidemia and cardiovascular disease. *Journal of Lipid Research* 53, 1723–1737. doi: 10.1194/jlr.R024794.

Preidis, G. A., Keaton, M. A., Campeau, P. M., Bessard, B. C., Conner, M. E., and Hotez, P. J. (2014). The Undernourished Neonatal Mouse Metabolome Reveals Evidence of Liver and Biliary Dysfunction, Inflammation, and Oxidative Stress. *The Journal of Nutrition* 144, 273–281. doi: 10.3945/jn.113.183731.

Qin, J., Li, Y., Cai, Z., Li, S., Zhu, J., Zhang, F., Liang, S., Zhang, W., Guan, Y., Shen, D., Peng, Y., Zhang, D., Jie, Z., Wu, W., Qin, Y., Xue, W., Li, J., Han, L., Lu, D., Wu, P., … Wang, J. (2012). A metagenome-wide association study of gut microbiota in type 2 diabetes. *Nature*, *490*(7418), 55–60. https://doi.org/10.1038/nature11450.

Ren, S., & Correia, M. A. (2000). Heme: a regulator of rat hepatic tryptophan 2,3-dioxygenase? *Archives of biochemistry and biophysics*, *377*(1), 195–203. https://doi.org/10.1006/abbi.2000.1755.

Roselli M, Schifano E, Guantario B, Zinno P, Uccelletti D, Devirgiliis C. (2019) Caenorhabditis Elegans and Probiotics Interactions from a Prolongevity Perspective. Int J Mol Sci.;20(20):5020. Published 2019 Oct 10. doi:10.3390/ijms20205020.

Scheithauer, T. P. M., Rampanelli, E., Nieuwdorp, M., Vallance, B. A., Verchere, C. B., van Raalte, D. H., et al. (2020). Gut Microbiota as a Trigger for Metabolic Inflammation in Obesity and Type 2 Diabetes. *Front. Immunol.* 11, 571731. doi: 10.3389/fimmu.2020.571731.

Schifano, E., Marazzato, M., Ammendolia, M. G., Zanni, E., Ricci, M., Comanducci, A., et al. (2019). Virulence behavior of uropathogenic *Escherichia coli* strains in the host model *Caenorhabditis elegans*. *MicrobiologyOpen* 8, e00756. doi: 10.1002/mbo3.756.

Schulz, T. J., Zarse, K., Voigt, A., Urban, N., Birringer, M., and Ristow, M. (2007). Glucose Restriction Extends Caenorhabditis elegans Life Span by Inducing Mitochondrial Respiration and Increasing Oxidative Stress. *Cell Metabolism* 6, 280–293. doi: 10.1016/j.cmet.2007.08.011.

Shen, J., Obin, M. S., and Zhao, L. (2013). The gut microbiota, obesity and insulin resistance. *Molecular Aspects of Medicine* 34, 39–58. doi: 10.1016/j.mam.2012.11.001.

Spanier, B., Lasch, K., Marsch, S., Benner, J., Liao, W., Hu, H., et al. (2009). How the Intestinal Peptide Transporter PEPT-1 Contributes to an Obesity Phenotype in Caenorhabditits elegans. *PLoS ONE* 4, e6279. doi: 10.1371/journal.pone.0006279.

Tawe, W. N., Eschbach, M.-L., Walter, R. D., and Henkle-Duhrsen, K. (1998). Identification of stress-responsive genes in Caenorhabditis elegans using RT-PCR differential display. *Nucleic Acids Research* 26, 1621–1627. doi: 10.1093/nar/26.7.1621.

Trefely, S., Lovell, C. D., Snyder, N. W., and Wellen, K. E. (2020). Compartmentalised acyl-CoA metabolism and roles in chromatin regulation. *Molecular Metabolism* 38, 100941. doi: 10.1016/j.molmet.2020.01.005.

Turnbaugh PJ, Ley RE, Mahowald MA, Magrini V, Mardis ER, Gordon JI. (2006) An obesity-associated gut microbiome with increased capacity for energy harvest. Nature. Dec 21;444(7122):1027-31. doi: 10.1038/nature05414.

van der Goot, A. T., and Nollen, E. A. A. (2013). Tryptophan metabolism: entering the field of ageing and age-related pathologies. *Trends in Molecular Medicine* 19, 336–344. doi: 10.1016/j.molmed.2013.02.007.

van der Goot, A. T., Zhu, W., Vázquez-Manrique, R. P., Seinstra, R. I., Dettmer, K., Michels, H., et al. (2012). Delaying ageing and the ageing-associated decline in protein homeostasis by inhibition of tryptophan degradation. *Proc. Natl. Acad. Sci. U.S.A.* 109, 14912–14917. doi: 10.1073/pnas.1203083109.

Van Gilst, M. R., Hadjivassiliou, H., and Yamamoto, K. R. (2005). A *Caenorhabditis elegans* nutrient response system partially dependent on nuclear receptor NHR-49. *Proc. Natl. Acad. Sci. U.S.A.* 102, 13496–13501. doi: 10.1073/pnas.0506234102.

Vernocchi, P., Gili, T., Conte, F., Del Chierico, F., Conta, G., Miccheli, A., et al. (2020). Network Analysis of Gut Microbiome and Metabolome to Discover Microbiota-Linked Biomarkers in Patients Affected by Non-Small Cell Lung Cancer. *IJMS* 21, 8730. doi: 10.3390/ijms21228730.

Vrablik, T. L., Petyuk, V. A., Larson, E. M., Smith, R. D., & Watts, J. L. (2015). Lipidomic and proteomic analysis of Caenorhabditis elegans lipid droplets and identification of ACS-4 as a lipid droplet-associated protein. *Biochimica et biophysica acta*, *1851*(10), 1337–1345. https://doi.org/10.1016/j.bbalip.2015.06.004.

Watts, J. L., & Browse, J. (2000). A palmitoyl-CoA-specific delta9 fatty acid desaturase from Caenorhabditis elegans. *Biochemical and biophysical research communications*, *272*(1), 263–269. https://doi.org/10.1006/bbrc.2000.2772.

Wishart, D. S. (2019). Metabolomics for Investigating Physiological and Pathophysiological Processes. *Physiological Reviews* 99, 1819–1875. doi: 10.1152/physrev.00035.2018.

Wu, Q., Ke, L., Wang, C., Fan, P., Wu, Z., and Xu, X. (2018). Global Analysis of Lysine 2-Hydroxyisobutyrylome upon SAHA Treatment and Its Relationship with Acetylation and Crotonylation. *J. Proteome Res.* 17, 3176–3183. doi: 10.1021/acs.jproteome.8b00289.

Xue, C., Qiao, Z., Chen, X., Cao, P., Liu, K., Liu, S., et al. (2020). Proteome-Wide Analyses Reveal the Diverse Functions of Lysine 2-Hydroxyisobutyrylation in Oryza sativa. *Rice* 13, 34. doi: 10.1186/s12284-020-00389-1.

Yen, K., Le, T. T., Bansal, A., Narasimhan, S. D., Cheng, J.-X., and Tissenbaum, H. A. (2010). A Comparative Study of Fat Storage Quantitation in Nematode Caenorhabditis elegans Using Label and Label-Free Methods. *PLoS ONE* 5, e12810. doi: 10.1371/journal.pone.0012810.

Zhao, X., Lu, L., Qi, Y., Li, M., & Zhou, L. (2017). Emodin extends lifespan of Caenorhabditis elegans through insulin/IGF-1 signaling pathway depending on DAF-16 and SIR-2.1. *Bioscience, biotechnology, and biochemistry*, *81*(10), 1908–1916. https://doi.org/10.1080/09168451.2017.1365592.

Zanni, E., Schifano, E., Motta, S., Sciubba, F., Palleschi, C., Mauri, P., et al. (2017). Combination of Metabolomic and Proteomic Analysis Revealed Different Features among Lactobacillus delbrueckii Subspecies bulgaricus and

lactis Strains While In Vivo Testing in the Model Organism Caenorhabditis elegans Highlighted Probiotic Properties. *Front. Microbiol.* 8, 1206. doi: 10.3389/fmicb.2017.01206.

Supplemental table and figures

act-1	FOR	5'-GAGCGTGGTTACTCTTTCA
	REV	5'-CAGAGCTTCTCCTTGATGTC
sek-1	FOR	5'-CAGAGCCGTTTATTGGGAAA
	REV	5'-TGCATCCGGCTTGTACAGT
sod-3	FOR	5'-AGAACCTTCAAAGGAGCTGATG
	REV	5'-CCGCAATAGTGATGTCAGAAAG
gst-4	FOR	5'-TCAATGTGCCTTACGAGGATTA
	REV	5'-CGAATTGTTCTCCATCGACTTG
daf-2	FOR	5'-ATCGTCGGATTCTACTGTACTCCC
	REV	5'-CCGACATCTGACAATATTCATTCTCGT
daf-16	FOR	5′-TCAAGACCTCAAAGCCAATCAACTC
	REV	5′-ACGAGAAAGAAGGAGTAAGAGGAGG
sams-1	FOR	5'-GAGAAGATGTCGGAGCAGGAGA
	REV	5'-TGTGGGAAAGAATGAGAGTCAATGG
sbp-1	FOR	5'-GGATGATATTGCGCCATTTC
	REV	5'- GGATCCGGTTGTTGTGATG
fat-7	FOR	5'-TGGCGGTAACGTGGCTCTCTTTG
	REV	5'-TAGGTCGAGTTTGCCTCCATGC
acs-2	FOR	5'-AGTGAGACTTGACAGTTCCG
	REV	5'-CTTGTAAGAGAGGAATGGCTC
tdo-2	FOR	5'-TCACAAAGTGGAGATACACCA
	REV	5'-CCTTCGTTCAACAGTCAGTGA

Table S1. Primers for real time qPCR analysis.

Metabolite	No-GD		HGD	
	CTRL	2-HIBA	CTRL	2-HIBA
Saturated fat	561.3±171.28	540.74±201.43	687.26±179.99	712.73±302.52
w-6	381.39±187.89	388.62±213.55	409.48±98.31	419.85±103.12
w-3	157.88±67.99	158.43±82.70	145.5±28.33	151.13±31.51
Monoacylglycerol	196.06±22.87	183.81±21.92	111.58±28.99	120.83±14.32
Triglycerides	124.49±57.42	124.57±61.30	191.23±63.23	194.82±84.64
Phospholipids	112.33±51.36	112.74±57.44	165.24±37.73	171.1±37.18
Val	29.30±21.16	31.34±21.81	29.55±8.36	31.46±11.49
Ile	18.59±14.38	18.75±14.39	20.92±8.20	23.57±9.61
Propionate	33.74±32.55	31.97±33.47	10.8±4.51	11.87±4.33
3-HIB	2.55±2.07	2.68±2.25	1.13±0.37	1.28±0.66
3-OH-but	6.29±4.14	5.98±4.83	3.99±2.45	4.35±2.61
3-OH-isoval	0.56±0.38	0.58±0.38	0.51±0.65	0.46±0.67
Ala	303.55±173.31	301.92±174.15	371.3±134.91	394.46±152.62
Lys	64.44±51.57	65.89±54.58	68.02±18.63	71.19±24.67
Acetate	75.52±27.64	68.53±25.27	58.85±10.61	66.4±12.98
Acetamide	19.00±11.74	20.56±11.69	22.68±6.65	23.78±6.53
N-acetyl-	9.17±6.80	9.00±7.50	3.71±1.07	3.70±0.95
5-aminopentanoic ac	25.75±15.76	24.35±16.56	41.41±28.62	46.52±33.44
Glu	83.06±48.73	88.15±56.64	89.69±36.66	93.24±34.76
Succinate	32.78±23.58	33.59±24.18	60.74±51.27	60.35±51.32
Gln	21.12±12.18	20.26±12.18	37.86±15.1	40.29±16.24
Phosphocholine	8.75±8.78	9.12±10.15	11.76±4.89	13.29±6.15
Choline	9.74±4.54	9.84±4.06	12.06±4.98	12.48±4.58
Betaine	6.33±4.68	6.55±5.71	8.18±4.19	8.05±3.11
Gly	34.45±26.45	34.96±26.25	160.56±62.22	176±79.75
Lactate	92.63±41.47	85.22±37.89	63.73±42.73	64.15±40.44
Glc	31.76±19.83	32.79±21.05	27.13±15.01	30.76±17.75
Threalose	32.67±16.92	33.15±17.08	60.34±52.59	70.06±66.3
U01	2.44±1.09	2.43±1.01	2.42±1.42	2.78±1.8
U02	2.60±0.90	2.64±0.76	4.90±2.67	5.31±3.61
CXP+UXP	23.25±16.77	22.99±16.07	25.06±6.34	27.35±8.34
Fumarate	0.46±0.47	0.39±0.42	2.29±1.16	2.30±0.85
His	15.16±8.82	14.23±9.24	14.26±4.4	16.15±7.02
Tyr	13.06±8.54	12.74±8.78	11.92±3.81	12.29±4.51
Phe	19.58±15.01	18.78±15	16.46±4.4	17.11±4.83
Trp	3.89±1.48	3.12±0.75	0.59±0.32	1.20±0.49
U03	8.99±6.98	5.96±4.44	5.84±1.79	6.54±4.30
GXP	8.20±7.43	8.01±7.55	10.17±2.88	11.14±2.04
U04	1.72±0.69	1.88±0.75	1.67±0.7	1.79±0.65
Formate	80.77±31.22	77.54±31.26	7.72±0.71	8.19±1.00
AXP	17.53±13.05	19.46±9.37	35.79±11.51	37.65±10.63
NamRib	2.66±2.06	2.78±1.99	1.79±0.89	2.16±1.56
NAD	2.32±0.77	2.25±0.82	2.79±1.10	2.82±1.06

Table S2. Metabolites mean and standard deviation. Data expressed as nmol/n, n= 1000 worms.

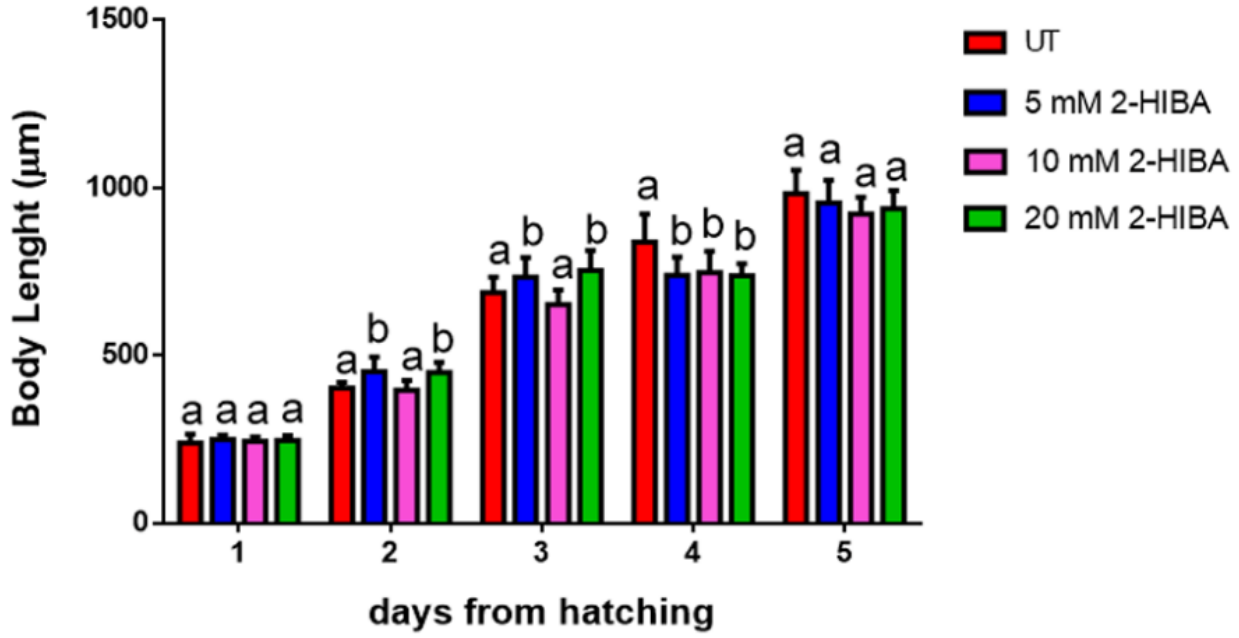

Figure S1. Analysis of body length in worms fed heat-killed OP50 supplemented with different concentrations of 2-HIBA. Length of worms during larval development was measured from head to tail at the indicated time points. UT: untreated worms. Different letters indicate statistically significant differences ($p < 0.05$).

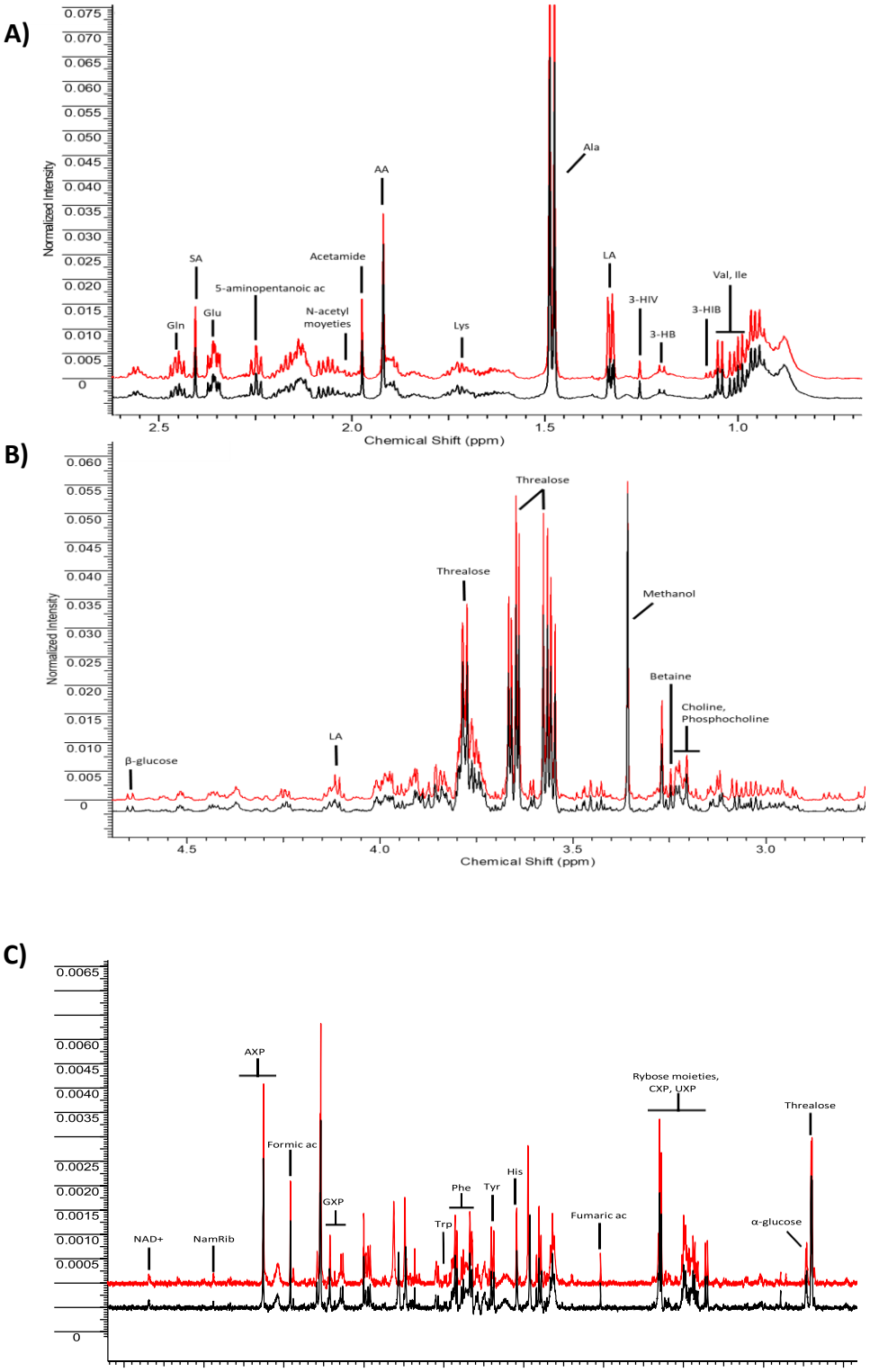

Figure S2. 600 MHz ^{1}H-NMR spectra of the *C. elegans* hydroalcoholic extracts in D_2O. Red spectrum: HGD worms supplemented with 2-HIBA 10 mM; black spectrum: untreated HGD worms.Regions: A) 0.5-2.5 ppm; B) 2.5-5.0 ppm; C) 5.0-9.5 ppm.

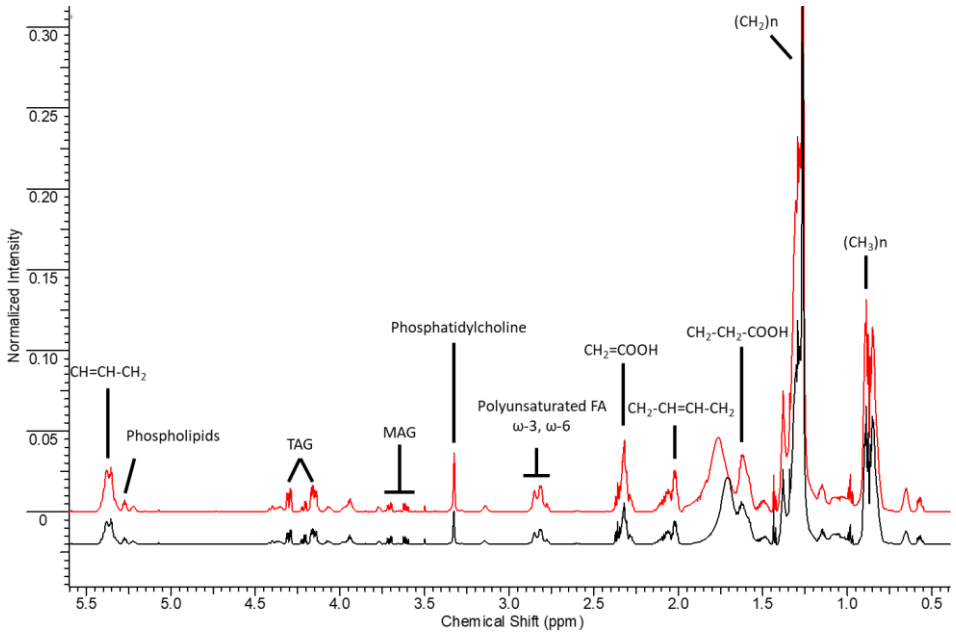

Figure S3. 600 MHz ^{1}H-NMR spectra of the *C. elegans* chloroformic extracts in CDCl3. Red spectrum: HGD worms supplemented with 2-HIBA 10 mM; black spectrum: untreated HGD worms.